United Aircraft Research Laboratories

U
UA
A

UNITED AIRCRAFT CORPORATION

EAST HARTFORD, CONNECTICUT

Report F-910375-2

Nuclear Criticality Studies of Specific
Nuclear Light Bulb and Open-Cycle Gaseous
Nuclear Rocket Engines

NASA Contract No. NASw-847

REPORTED BY _T. S. Latham_

T. S. Latham

APPROVED BY _J. L. Cooley_

J. L. Cooley
Chief, Systems Analysis Section

DATE September 1967

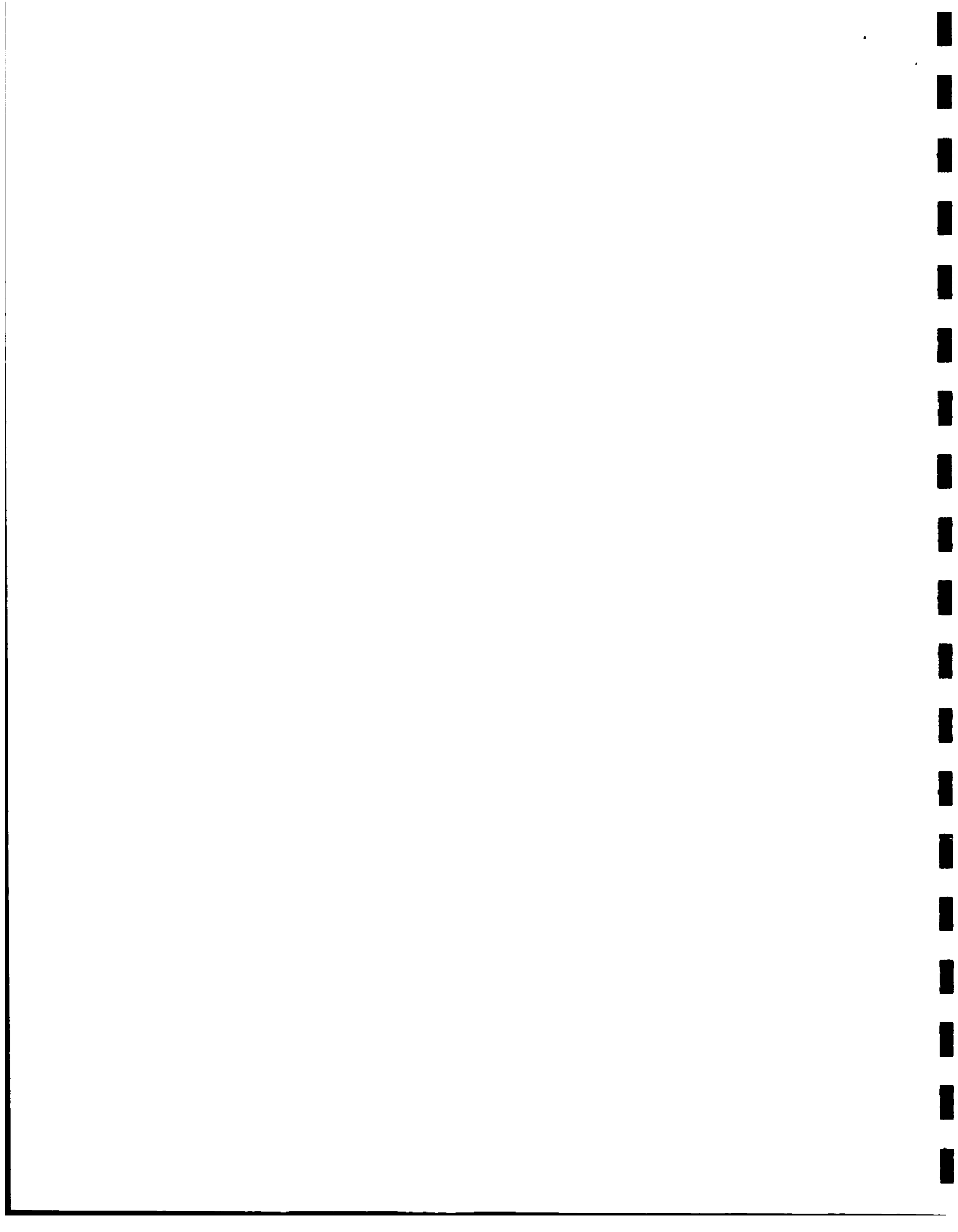NO. OF PAGES 52   COPY NO. 9

FOREWORD

An exploratory experimental and theoretical investigation of gaseous nuclear rocket technology is being conducted by the United Aircraft Corporation Research Laboratories under Contract NASw-847 with the joint AEC-NASA Space Nuclear Propulsion Office. The Technical Supervisor of the Contract for NASA was Captain W. A. Yingling (USAF) for the first portion of the contract performance period and was Captain C. E. Franklin (USAF) for the last portion of the contract performance period. Results of portions of the investigation conducted during the period between September 15, 1965 and September 15, 1967 are described in the following six reports (including the present report) which comprise the required sixth Interim Summary Technical Report under the Contract:

1. Travers, A.: Experimental Investigation of Radial-Inflow Vortexes in Jet-Injection and Rotating-Peripheral-Wall Water Vortex Tubes. United Aircraft Research Laboratories Report F-910091-14, September 1967.

2. Kendall, J. S.: Experimental Investigation of Heavy-Gas Containment in Constant-Temperature Radial-Inflow Vortexes. United Aircraft Research Laboratories Report F-910091-15, September 1967.

3. Douglas, F. C., R. Gagosz, and M. A. DeCrescente: Optical Absorption in Transparent Materials Following High-Temperature Reactor Irradiation. United Research Laboratories Report F-910485-2, September 1967.

4. Gagosz, R., J. Waters, F. C. Douglas, and M. A. DeCrescente: Optical Absorption in Fused Silica During TRIGA Reactor Pulse Irradiations. United Aircraft Research Laboratories Report F-910485-1, September 1967.

5. Latham, T. S.: Nuclear Criticality Studies of Specific Nuclear Light Bulb and Open-Cycle Gaseous Nuclear Rocket Engines. United Aircraft Research Laboratories Report F-910375-2, September 1967. (present report)

6. McLafferty, G. H. and H. E. Bauer: Studies of Specific Nuclear Light Bulb and Open-Cycle Vortex-Stabilized Gaseous Nuclear Rocket Engines. United Aircraft Research Laboratories Report F-910093-37, September 1967.

Report F-910375-2

Nuclear Criticality Studies of Specific Nuclear Light Bulb and Open-Cycle Gaseous Nuclear Rocket Engines

TABLE OF CONTENTS

Nuclear Criticality Studies of Specific Nuclear Light Bulb

and Open-Cycle Gaseous Nuclear Rocket Engines

SUMMARY

Analytical studies were conducted to determine the U-233 critical mass requirements for two specific vortex-stabilized gaseous nuclear rocket engines: a nuclear light bulb engine and an open-cycle engine. The specific open-cycle engine employs a single cylindrical cavity having both a length and a diameter of 6 ft. The specific nuclear light bulb engine employs seven separate cavities, each having a length of 6 ft; the total volume of all seven cavities approximately equals the volume of the single cavity of the open-cycle engine. The nuclear light bulb engine employs beryllium oxide between the unit cavities, layers of beryllium oxide and graphite surrounding the assembly of seven unit cavities, a relatively large amount of neutron-absorbing structural material in the end walls, seven separate exhaust nozzles, fuel and propellant injection ducts, and hot gases in the propellant and fuel regions. The open-cycle engine employs layers of beryllium oxide, graphite, and heavy water surrounding the cavity; various structural materials; an annular exhaust nozzle; fuel and propellant injection ducts; and hot gases in the propellant and fuel regions.

Studies were also made to determine the effect on criticality of various modifications to a reference configuration for each of the specific engines. For the nuclear light bulb engine, these included addition of impurities to the moderator materials, changes in the end-wall portions of the moderator, and changes in material and gas temperatures. For the open-cycle engine, these included changes in the nozzle-approach configuration, changes in the cavity liner materials, elimination of heavy water from the reflector-moderator, and substitution of hydrogen for helium in the moderator coolant circuit.

The analyses of the nuclear light bulb engine were made using 4-group two-dimensional transport theory and 24-group one-dimensional transport theory. The analyses of the open-cycle engine were made using 4-group two-dimensional diffusion theory and 24-group one-dimensional diffusion and transport theories.

RESULTS AND CONCLUSIONS

Nuclear Light Bulb Engine

1. A U-233 critical mass of 43.5 lb was determined for the reference configuration on the basis of two-dimensional neutron transport theory.

2. The addition of specified impurities to the beryllium oxide and graphite moderator materials caused an increase in critical mass of approximately 35% relative to the reference configuration.

3. The critical mass could be reduced substantially by a reduction in the amount of neutron-absorbing materials in the end walls and nozzle-approach regions, since the macroscopic neutron-absorption cross section of these materials is approximately ten times that for the impurities introduced into the moderator materials.

4. Replacement of graphite in the upper and lower end walls and the nozzle-approach regions by equal volumes of beryllium oxide caused a decrease in critical mass of approximately 6% relative to the reference configuration.

5. A doubling of the mass of beryllium oxide in the lower-end-wall and nozzle-approach regions caused a decrease in critical mass of approximately 12% relative to the reference configuration.

6. Changes in moderator and gas temperatures resulted in relatively large changes in critical mass in some instances on the basis of one-dimensional transport theory.

Open-Cycle Engine

7. A U-233 critical mass of 43.1 lb was determined for the reference configuration on the basis of two-dimensional diffusion theory. (This critical mass is 14% less than that calculated in a preceding study in which the volume of the exhaust-nozzle approach slot was twice that for the reference configuration.)

8. The critical mass was reduced 12% relative to the reference configuration as a result of the following modifications: replacement of the tungsten liner tubes with NbC-coated, pyrolytic-graphite-insulated, beryllium tubes; elimination of the heavy-water moderator; and substitution of hydrogen for helium in the moderator coolant circuit.

INTRODUCTION

The Research Laboratories of United Aircraft Corporation are investigating various aspects of gaseous nuclear rocket technology under Contract NASw-847 with the joint AEC-NASA Space Nuclear Propulsion Office. These investigations have application to determining the feasibility of two different vortex-stabilized gaseous nuclear rocket engine concepts: a nuclear light bulb engine concept and an open-cycle engine concept. Both engine concepts are based on the transfer of energy by thermal radiation to seeded hydrogen propellant from gaseous nuclear fuel suspended in a vortex. The open-cycle engine employs a vortex driven by the tangential injection of propellant flow and relies entirely on fluid circulation phenomena for preferential fuel containment. The nuclear light bulb engine employs an internally-cooled transparent wall between the fuel-containment and propellant regions, and employs a vortex driven by tangential neon injection to provide a buffer region between the fuel and the transparent wall. The nuclear light bulb concept offers the potential of perfect containment of fuel and fission products. From a geometrical point of view, the two engine concepts differ in that the open-cycle engine employs a single cavity, while the nuclear light bulb engine appears to be more practical in a seven-cavity configuration.

The work under Contract NASw-847 has included investigations of the fluid mechanics of vortex flow, radiant heat transfer, and radiation damage to transparent materials. Also included are analytical investigations to provide information needed to interpret the results of the other investigations in terms of the performance of full-scale engines. Initial criticality studies of full-scale engines were devoted to the open-cycle engine (Ref. 1). However, results of fluid mechanics studies obtained early in 1967, along with interpretation of these results in terms of the fuel loss rates in full-scale engines (Ref. 2), indicated that the fuel loss rates in the open-cycle engine would be too great for economical engine operation. As a result, the emphasis in the studies described in the present report was shifted from the open-cycle engine to the nuclear light bulb engine early in 1967. However, the present report includes the results of the criticality work on the open-cycle engine because of the possible application of these results to other engine concepts.

Calculations of critical masses required in cavity reactors were reported first in Refs. 3 and 4, and further work has been reported in Refs. 5 through 14. Experimental measurements of critical mass requirements for selected cavity reactor configurations are reported in Refs. 15 through 17. In most instances, both the analytical work and the experimental measurements were made for idealized spherical cavities or for cylindrical configurations with length-to-diameter ratios of 1.0. Moderator materials employed for these measurements and calculations were also ideal (no voids for coolant or propellant passage and no structural materials) and were graphite, beryllium oxide, heavy water, or combinations of these three containing little or no neutron poisons. However, some calculations and measurements

have been performed which include factors which should be considered in cavity reactors for nuclear rocket applications. In particular, calculations have been made which include the effects on critical mass resulting from the addition of heat- and pressure-resistant lining materials on the inner cavity wall (Refs. 1, 7, 9, 10, and 14) and by the presence of an exhaust nozzle penetrating the reflector-moderator (Refs. 1, 8, and 9). Experimental measurements have been made of the effects of an exhaust nozzle penetrating the reflector-moderator of a heavy-water-reflected cavity (Refs. 15 and 17). In the recent experiments of Ref. 17, measurements were also made of the effects of the following: variation in fuel radius; variation in heavy water temperature; insertion of a simulated fuel injection duct; the presence of a steel cavity wall liner; and the addition of beryllium moderator at different radial locations within the heavy-water reflector-moderator. Additional calculations have been performed to estimate the effects of hot hydrogen on the neutron spectra and critical masses for cavity reactors (Refs. 1 and 12). Critical mass require- ments were calculated in Ref. 1 for a specific engine design which includes coolant voids, plumbing structure, cavity lining material, exhaust nozzle holes penetrating the reflector-moderator and pressure vessel, hot hydrogen, a specific fuel density profile, and a fuel injection duct surrounded by a sleeve made of a strong neutron poison to prevent excessive heating of the fuel and local moderator volume during fuel injection. The nuclear calculations in the present report for the open-cycle engine are extensions of the work reported in Ref. 1. The calculations for the nuclear light bulb engine are made for an integrated cluster of seven unit cavities, amounting essentially to a large cavity reactor with internal moderation. The object of the present study is to establish the critical mass of a reasonable geometrical configuration with proper simulation of exhaust nozzle geometry, hot propellant gases, neutron poisons due to structural and plumbing materials, and moderator volume fractions. In addition, attempts are made to establish a method for calculating few-group cross sections from one-dimensional multigroup results which can be used with confidence in two-dimensional calculations. Finally, attempts are also made in the present study to establish reliable buckling correction factors so that investigation of the effects of changes in parameters such as moderator temperature can be performed using the more economical one-dimensional codes.

NUCLEAR LIGHT BULB ENGINE

Specifications and Nuclear Configurations

The nuclear light bulb engine design used as a basis for nuclear criticality calculations is described in Ref. 2, and a preliminary layout of the engine is shown in Fig. 4 of Ref. 2. The configuration used to approximate the compositions, dimensions, and geometry of the conceptual engine design for nuclear calculations was obtained from an early configuration considered in the studies described in Ref. 2, but agrees in essential details with the final design with the following exceptions: (1) a pressure vessel made of steel instead of a glass-fiber-wound pressure vessel was used for the nuclear calculations, and (2) substantially greater masses of natural tungsten and steel were present in the lower and upper end walls and in the nozzle-approach regions for the nuclear calculations than were employed in the final design of Ref. 2. The effect on critical mass of replacing a steel pressure vessel with a fiber-wound pressure vessel should be negligible. However, the presence of substantially greater masses of natural tungsten and steel in the upper and lower end walls and in the nozzle-approach regions does have a large effect on the critical mass because the relatively large amount of thermal neutron absorption seriously reduces the neutron reflection efficiency in both end walls.

Figure 1 shows the basic cylindrical geometry used for two-dimensional calculations of the nuclear light bulb engine. Details of the dimensions and temperatures of the various regions and the number of radial and axial mesh points employed in both one-dimensional and two-dimensional calculations for this configuration are contained in Table I.

In order to describe the characteristics of the fuel regions of the nuclear light bulb engine, it was necessary to develop a unit cell in which the fuel regions and the various layers of hot gases and transparent wall were described in detail. A cross section of a detailed unit cell is shown in Fig. 2, and the dimensions and composition of materials employed in the detailed unit cell are contained in Tables II and III.

Previous experience with the calculation of U-233 critical masses in spherical assemblies (Ref. 12) has indicated that critical masses are relatively insensitive to homogenization and the resulting uniform distribution of the fuel and hot gases throughout the cavity. Therefore, in order to save computation time in two-dimensional transport theory calculations, it was decided to homogenize the unit cell by volume-weighting each of the ten principal regions.

Additional regions which were homogenized to reduce computation time in two-dimensional calculations include the structure and plumbing region above the upper end wall, the upper end wall, the lower end walls, and the nozzle-approach regions.

The structure and plumbing, region 20 of Fig. 1, contains a steel structural plate to carry the gravitational load of the reactor core, hafnium fuel injection ducts, pumps, heat exchangers, and piping containing propellant and coolant fluids. In addition, unoccupied portions of region 20 are pressurized with hydrogen to 500 atm. The upper end wall, region 21 of Fig. 1, contains graphite or BeO and various manifolds for coolant and propellant, plus hafnium fuel injection ducts. The nozzle approaches, regions 22 and 23 of Fig. 1, contain the hot gases being expelled through the nozzle, plus the nozzle-approach liner material, and natural tungsten supports for the graphite or BeO end plugs at the ends of the unit cells. The lower end walls, regions 24 to 27 of Fig. 1, contain additional plumbing and manifolding structure as well as some graphite or BeO moderating material in interstitial zones. Since the end plugs at the end of the unit cells, shown in Figs. 4 and 5 of Ref. 2, were of a larger diameter than the fuel-containing region, it was felt that homogenization of the nozzle approach did not substantially alter the neutron leakage characteristics through that region. Homogenization of the other zones mentioned above should not affect the accuracy of calculations of the nuclear characteristics of the system to any substantial degree.

Table IV contains the composition of all of the various regions employed for both one- and two-dimensional calculations for the nuclear light bulb engine. Figure 3 shows the cross section at the mid-plane of the nuclear light bulb engine employed for all one-dimensional calculations. Table V gives a summary of the various configurations which were used for the nuclear calculations and includes several variations in the configuration, principally due to the replacement of graphite with BeO in various amounts in the end walls and nozzle approaches. The densities and total masses of materials employed in the two-dimensional con-figuration are contained in Table VI. The weights of materials employed are in substantial agreement with those listed in Table X of Ref. 2 with the previously mentioned exceptions of replacement of the steel pressure vessel with a fiber-wound shell and removal of large quantities of natural tungsten and steel, both parasitic neutron absorbers, from the end-wall and nozzle-approach regions.

Steps in Analysis

The configuration used for nuclear calculations which has been described in the preceeding section includes adjacent zones with widely differing neutron scattering and absorption properties. Such a configuration requires a large number of mesh points for two-dimensional neutron transport theory calculations. Therefore, in order to remain within the limits of reasonable computation time, the following steps were followed in the nuclear analysis.

First, the minimum order of angular quadrature was established by performing a series of one-dimensional, infinite-cylinder calculations for the detailed unit

cell described in Tables II and III and Fig. 2. The DTF-II code (Ref. 18) was used for these calculations, and the results indicated that fluxes and eigenvalues remained essentially the same for S4, S6, and S8 angular quadrature. It was decided on this basis to use S4 angular quadrature for all succeeding calculations.

There was also a need to minimize the number of neutron energy groups and, if possible, eliminate the use of up-scattering cross sections from the two-dimensional calculations. This task was accomplished by performing one-dimensional, infinite-cylinder calculations using 24 neutron energy groups with down-scatter to 11 groups and up-scatter to 13 groups for configurations A and B of Table V. The ANISN code (Ref. 19) was used for these calculations, and the option which calculates flux- and volume-weighted few-group cross sections was employed to produce a 4-group cross section set. Up-scatter was removed by employing the additional option in the few-group calculations by the ANISN code which accomplishes removal of up-scatter by modification of the down-scatter cross sections in a manner which conserves the net transfer of neutrons. To ensure the accuracy of the 4-group cross sections, they were reused in calculations for the same one-dimensional configuration from which they were generated, and comparisons of eigenvalues, fluxes, leakages, and absorptions by region were made with the original 24-group results.

Two-dimensional calculations were carried out for configurations D through J described in Table V using the 4-group cross sections and S4 angular quadrature in the DOT code (Ref. 20).

In order to perform additional exploratory calculations economically, such as computation of the variation of critical mass with moderator temperature, it was necessary to establish a buckling correction for the one-dimensional cylindrical configuration C of Table V such that critical fuel loadings and radial neutron flux distributions would duplicate accurately those from the corresponding two-dimensional results. Once this buckling correction was established in the form of an effective cylinder height, the above-mentioned exploratory calculations were carried out using the one-dimensional ANISN code with 24 neutron energy groups.

Neutron Cross Sections

It was necessary to employ several thermal neutron energy groups in the range from 0 to 1.125 ev in order to calculate the neutron absorptions and spectra accurately for adjacent regions in the moderator at quite different temperatures. In addition, in order to calculate the effects of neutron up-scattering by the presence of hydrogen and hot neon in temperatures ranges from 2000 to 12,000 R in the gaseous fuel regions, it was also necesary to add several thermal neutron energy groups in the range between 1 and 29 ev. The basic set of 24 neutron energy groups was chosen with 14 of the groups covering the range from 0 to 29 ev and the remaining groups covering the range from 29 to 10^7 ev. Table VII contains the energy boundaries of the 24-group structure.

The fast neutron cross sections were calculated using the GAM-I code (Ref. 21) with slowing-down spectra calculated for the various local moderator materials. The slowing-down spectrum in the cavity regions was assumed to be that of the beryllium oxide moderator, the material in largest quantity adjacent to the cavities.

Thermal neutron absorption cross sections were calculated using the TEMPEST code (Ref. 22) with the spectra again chosen for the temperatures and materials of the local moderator regions. Up- and down-scattering probabilities within the thermal neutron energy groups were calculated using the SOPHIST-I code (Ref. 23). The SOPHIST-I code includes in the up- and down-scattering probabilities the enhancement of reaction rates due to relative velocity between the neutron and the scatterer; this effect was included in the calculation of the transport cross sections for the various materials.

Treatment of the transport cross section in the special cases of atomic and molecular hydrogen and hot neon follows that reported in Ref. 1 with the addition of dependence of the scattering cross section of molecular hydrogen on the energy of interaction, a function of relative velocity. The equation for the transport cross section is given below.

$$\sigma_{tr}^i = \sigma_a^i + (\sum_{j=1}^{13} \mu_{ij}) \; \sigma_s^i \; (1-\overline{\cos\theta})_i \tag{1}$$

The sum of μ_{ij} is the sum of the up- and down-scattering probabilities for energy group i to all energy groups j, $\overline{\cos\theta}$ is the mean value of the cosine of the scattering angle (which includes consideration of the motion of the scatterer as well as the incident neutron as described in Ref. 1), and σ_s^i allows for the relative velocity dependence necessary to correct for the effects of molecular binding on the scattering cross section at low interaction energies.

In order to calculate two-dimensional configurations economically, the 24-group cross sections used in the one-dimensional infinite-cylinder calculations were used to generate volume- and flux-weighted 4-group cross sections. The neutron energy boundaries of the 4-group set are also shown in Table VII. The boundary between groups 3 and 4 in the 4-group set is at 8.32 ev, and some up-scattering of neutrons from group 4 to group 3 did occur. In order to eliminate up-scattering probabilities from the two-dimensional problems, the option in the ANISN code (Ref. 19) which subtracts the up-scattering from the down-scattering and thereby maintains the balance of transfer of neutrons between adjacent groups was used to create a 4-group cross section set which had only down-scattering.

To evaluate this technique for generating 4-group cross sections in the one-dimensional case, companion problems were run for the cylindrical configuration A of Table V using first the 24-group set and then the 4-group set generated from the 24-group calculation. Table VIII contains comparisons of effective multiplication factors, absorptions, and leakages by region between these two calculations. It can be seen that the multiplication factor was reproduced very accurately and that there is close correspondence between absorptions, leakages, and integrated fluxes by regions for each of the 4 energy groups. The close correspondence between the 24- and 4-group calculations for identical configurations created confidence in the use of the 4-group cross sections for two-dimensional calculations.

Results of Initial One-Dimensional Calculations

The initial one-dimensional calculations were carried out using the 24-group cross section set and S4 angular quadrature in the ANISN neutron transport theory code. Using a U-233 fuel loading equivalent to 22.2 lb in the two-dimensional configuration, K_{eff}'s of 0.966 and 1.169 were calculated for the infinite cylindrical configurations A and B of Table V, respectively. Configuration A had impurities in the BeO and graphite moderator materials, while configuration B did not. The 20% reduction in K_{eff} due to the presence of impurities demonstrates the sensitivity of cavity reactor systems to parasitic neutron absorbers. Table IX contains a listing of the impurities included in the BeO and graphite.

The fluxes and volumes from these calculations were used to produce weighted 4-group cross sections as described previously. The comparisons between 4-group and 24-group calculations have also been mentioned previously and are shown in Table VIII.

Figure 4 contains a comparison of integrated fluxes from the calculation for configuration A in the two fuel regions and the intervening beryllium oxide. It can be seen that the inner fuel region has a softer spectrum than the outer fuel region in this configuration. This difference occurs because approximately 80% of the fission neutron source originates in the outer fuel region, and the fission neutrons must traverse and be moderated by the intervening BeO zone before entering the inner fuel region. It can also be seen that the presence of the moderator between the two fuel regions tends to soften the flux considerably, since the inner BeO flux spectrum is softer than either of the fuel spectra.

In the interest of equalizing power output per unit cell, it is evident that some of the inner BeO may have to be moved to the outer BeO region in later design variations because the fission neutron source and integrated flux per unit cell are approximately 1.5 times larger in the central fuel cell than in the six outer fuel cells.

Results of Two-Dimensional Calculations

Two-dimensional, 4-group, S4 neutron transport theory calculations were carried out using the DOT code (Ref. 20) to determine the critical masses of several two-dimensional configurations. The reference configuration is that described by Tables I to IV and Fig. 1. Table V contains a listing of variations in the basic configuration which were examined. These variations included the use of BeO and graphite moderator both with and without impurities, the removal of hafnium fuel injection ducts from the upper end wall and structural support regions, the replacement of graphite by an equal volume of BeO in both the upper and lower end walls and nozzle approaches, and then a doubling of the BeO mass in the lower end-wall and nozzle approaches. The results of these calculations are summarized in the last column of Table V and are shown graphically in Fig. 5 for configurations without impurities and in Fig. 6 for configurations with impurities.

It can be seen that the inclusion of impurities in the principal moderator regions has a drastic effect on the U-233 critical mass, increasing the critical mass from 43.5 lb for the reference configuration (configuration D) to 58.3 lb for configuration E, and causing increases of similar magnitude in changing from configurations G to H and I to J. The tremendous sensitivity to impurities is characteristic of cavity reactors; however, the particular configurations under study are even more sensitive to impurities due to the large loss of neutrons to both end reflectors. Replacing the original graphite end-wall material with Beo reduces the U-233 critical mass as does a doubling of the volume of BeO placed in the lower end wall and in the nozzle approaches; the final change yields the lowest critical mass requirement of 38.3 lb with no impurities in the moderator materials. Linear interpolation indicates that the BeO material coefficients $(\Delta M/M_c)/\Delta M_{BeO}$ for the nozzle approaches and lower end wall are -8.145 x 10^{-6} lb^{-1} and -7.344 x 10^{-6} lb^{-1} for configurations with and without impurities, respectively.

The removal of the hafnium fuel injection ducts was considered only in configuration F in which impurities were present in the moderator regions. In this case, the removal of the hafnium ducts caused little change in critical mass. Linear interpolation indicates that the Hf material coefficient, $(\Delta M/M_c)/\Delta M_{Hf}$ is 1.767 x 10^{-3} lb^{-1}. The choice of the total hafnium weight required to surround the fuel injection ducts to prevent melting or vaporization of the fuel during injection was based on the results of Ref. 24. The effect of the presence of hafnium in the present configuration is small, possibly because of the large amount of poison due to structural materials in the end walls (see Table X). The addition of hafnium to a configuration in which the amount of neutron poisons was initially lower is much greater (Ref. 24) because of the resulting increased neutron flux in the end-wall regions.

In order to illustrate the relative importance of impurities in the beryllium oxide and graphite and the effects of heavy absorbers such as natural tungsten

and steel in the end walls, Table X was constructed to contain a summary of the absorption characteristics in the moderator and cell regions of the nuclear light bulb engine. It can be seen from this table that the presence of impurities causes more than a four-fold increase in the macroscopic absorption cross section of these principal moderating materials. Further examination of the absorption character- istics in the end-wall regions of the two-dimensional nuclear light bulb con- figurations indicate that the presence of steel and natural tungsten causes the macroscopic absorption cross sections in these regions to be about ten times greater than the absorption in the impure moderator materials. The absorptions by tungsten and steel in the end walls and nozzle approaches is so dominant that little change is apparent in the macroscopic cross sections of these regions when impurities are removed from the BeO or graphite. This would indicate that the region thickness measured in absorption mean-free-paths of the end-wall materials would cause the end walls to have little or no effect in reflecting neutrons back into the system. This is the principal reason for the critical masses being as high as they are and, in addition, generally higher than the critical masses for a single cavity. This result is contrary to the expected result in which internal moderation should lower the critical fuel loading for a cavity reactor. Preliminary diffusion theory cal- culations indicate that slight internal moderation should cause critical masses to be approximately 25% lower than those required for a single cavity of equal volume. Of particular note is the rather high neutron absorption in the nozzle-approach regions. This is due principally to the rather heavy tungsten structural materials which were placed in the nozzle-approach regions to support the end plug in an early engine design conceived prior to the final design of Ref. 2. The total absorbing area in the end-wall and nozzle-approach regions is approximately ten times that added by the impurities shown in Table IX. Therefore, a reduction in the mass of the structural materials in these regions should result in a large reduction in critical mass. The magnitude of this reduction will require a reassessment of the amount of structural materials required in these regions.

Results of Additional One-Dimensional Calculations

One-dimensional, 24-group, $S4$ neutron transport calculations were performed to establish an equivalent height to be employed in the one-dimensional calcula- tion to simulate two-dimensional results for configuration I. In these calculations, 38.3 lb of U-233 were placed in the fuel regions and the height of the cylinder was varied until a value of K_{eff} of 1.0 was reached. When this height was established at 268.5 cm (see Fig. 7), a 4-group calculation was made with the same one-dimensional geometry, configuration C of Table V, to compare the 4-group and 24-group results. The K_{eff}'s for the 4- and 24-group cases were 0.999730 and 1.006654, respectively.

An additional result from the one-dimensional calculations was the computation of the fast neutron spectrum in the vicinity of the transparent wall within the unit cell. This spectrum is of interest in determining the effects of radiation

damage on the transmission characteristics of the transparent wall to the block-
body thermal radiation from the hot fuel cloud. Table XI contains the integrated
neutron flux above 0.111 Mev in the transparent wall region calculated for nuclear
light bulb engine configuration C. Two columns of flux are included in Table XI,
one for the neutron flux normalized to a production in the fuel region of 1 neutron
per second, and the other for the neutron flux normalized to a nominal power level
of 4600 Mw (see Ref. 2).

Using the established effective height for configuration C of 268.5 cm, the
behavior of the critical mass resulting from variations in temperature and hot gas
temperatures was examined. The first two variations in temperature were changes
in the BeO and graphite temperatures of ±10% about the normal operating conditions
with no other accompanying changes in the system. The results of these calculations
are shown in Table XII and indicate a relatively small effect on critical mass due
to small changes in moderator temperature.

Another calculation was made in which the graphite and BeO temperatures were
halved, and the hot hydrogen in region 8 of the fuel region was reduced in
temperature from 12,000 R to 8000 R. For the constant fuel loading of 38.3 lb,
K_{eff} dropped to 0.846, and the required critical mass rose to 59.6 lb. The reason
for this large increase in mass can be shown by examining Table XIII which contains
average cross sections in group 4 for the various materials used under these
variations in temperature. The table indicates that the absorption of the fuel
changed upward slightly from 2.56×10^{-3} cm^{-1} to 2.73×10^{-3} cm^{-1} with the decrease in
temperature to half the normal operating level, while the moderator absorptions
increased with approximately $(1/T)^{1/2}$ dependence. Thus, the thermal utilization
of the system grew worse with the particular temperature change of the moderating
material. It should also be noted that, between the temperatures of 2533 and 1265 R
for beryllium oxide, $\nu\Sigma_f$ for U-233 rises only slightly from 4.84×10^{-3} to 5.10×10^{-3}
cm^{-1}. The combination of these effects causes the increase in critical mass.

The final one-dimensional calculation was carried out for the case in which all
of the materials in the reactor were at room temperature, 540 R. In this case, for
constant fuel loading of 38.3 lb of U-233, K_{eff} rose to 1.087, while the critical
mass decreased to 27.6 lb. In this instance, while the moderator absorption
increased approximately as $(1/T)^{1/2}$, $\nu\Sigma_f$ and absorption in the fuel regions also
rose drastically above that for the case where the moderator temperatures were
1265 R. $\nu\Sigma_f$ rose to $8.77 \times 10^{-3} cm^{-1}$ while Σ_a in the fuel region rose from
2.73×10^{-3} to 4.01×10^{-3}. The trends indicating this variation can also be seen
in variations of cross sections shown in Table XIII.

Flux Plots for One- and Two-Dimensional Calculations

Radial mid-plane neutron flux plots from both one- and two-dimensional 4-group,
S4 calculations are compared in Fig. 8. These calculations were done for

configuration I which had twice the mass and volume of BeO in the lower end wall and nozzle approach regions than was used in configuration D. It can be seen from these flux plots for groups 3 and 4 that the shapes of the radial flux plots are very similar for both groups with the fluxes being slightly higher for the one-dimensional cylindrical assembly than for the two-dimensional case. Features to note in these flux plots are the buildup of thermal flux in the beryllium oxide moderator regions, the much higher flux level in the central unit cell, and the apparent self shielding in group 4 in both the central cell and in the outer fuel region. The phrase "apparent self shielding" is used because it is the large effective scattering cross section of the hot gases, $(\Sigma_{tr} \cong 30\Sigma_a$ in the fuel regions) rather than absorption which creates a diffusion barrier for group-4 neutrons in the fuel region. This effective self shielding due to scattering may cause additional increases in critical mass when more detailed calculations of the unit cell described in Tables II and III and Fig. 2 are performed.

Figure 9 contains flux plots for all four energy groups from two-dimensional critical mass calculations for configuration H. These flux plots are at the radial mid-plane and contain essentially the features discussed in the previous plots of Fig. 8. Figure 10 contains axial neutron flux plots down the centerline of the two-dimensional configuration H. The principal feature to be noted here is the large amount of leakage into the end walls in all groups, indicating the relative ineffectiveness of the end walls in reflecting neutrons back into the system. It is expected that removal of the heavy absorption by natural tungsten and steel in the end-wall regions will improve the reflecting properties to the extent that the group-4 flux will build up in these regions rather than follow the outward axial leakage of other energy groups.

Figure 11 contains radial neutron flux plots through the nozzle-approach regions. The principal characteristics to be noted are the peaking of the groups 3 and 4 fluxes in the moderator regions and the peaking of the groups 1 and 2 fluxes in the nozzle-approach regions, indicating continuing neutron moderation in the lower end wall and nozzle approaches and some streaming of fast neutrons through the nozzle approaches and nozzle throats. It should be noted, however, that the magnitudes of the fluxes in this region, especially in the nozzle-approach region, are an order of magnitude below those in the fuel region.

Figure 12 contains radial neutron flux plots through the nozzle throat regions. Once, again, the groups 1 and 2 fluxes are peaked over the nozzle throat regions, while the groups 3 and 4 fluxes are relatively flat and behave as though they were in a homogenous moderator region. It should be noted here also that the fluxes in these regions are two orders of magnitude lower than those in the fuel region.

OPEN-CYCLE ENGINE CRITICALITY CALCULATIONS

Criticality calculations were made for a modified version of the engine design of Refs. 1 and 25 in which the size of the exhaust nozzle approach slot was reduced by 50%. Two-dimensional diffusion theory calculations using the TWENTY GRAND code (Ref. 26) indicated a critical mass for this configuration of 43.1 lb of U-233 relative to a value of 50.1 lb for the configuration with the larger nozzle-approach region in Ref. 1. This mass of 43.1 lb compares well with a predicted mass of 42.2 lb from Ref. 1 which was based on interpolation from other configurations.

Three additional changes to the specific gaseous nuclear rocket configuration as presented in Refs. 1 and 25 were investigated to determine their effects on critical mass. These modifications were: 1) replacement of the tungsten liner tubes with pyrolytic-graphite-coated beryllium tubes, 2) elimination of the heavy water moderator, and 3) substitution of hydrogen for helium in the moderator coolant circuit. Using the equivalent spherical geometry employed in Ref. 1, one-dimensional, 24-Group, neutron transport theory and diffusion theory calculations were performed for this particular configuration incorporating all three of the above changes. S4 angular quadrature in the neutron transport theory calculations was determined to be sufficient for the spherical configuration by the same procedure employed for the nuclear light bulb calculations. Figure 13 shows the geometry of this spherical assembly. Tables XIV and XV contain the dimensions and compositions employed in the various regions of the spherical assembly. The results of these calculations are shown in Figs. 14 and 15. In Fig. 14, the integrated neutron fluxes from the transport theory calculations in the regions in the center of the sphere and in the moderator regions are shown. It can be seen that the effects of the very hot hydrogen at 100,000 R cause the spectrum to become very hard in the center fuel region, region 2. It can also be seen that the relatively narrow region of cool hydrogen in region 5 causes the spectrum to soften considerably and that the beryllium oxide innermost reflector-moderator causes the spectrum to be softer than in all of the other three regions.

Figure 15 contains the results of several one-dimensional calculations. Preliminary diffusion theory calculations were made using the ULCER code (Ref. 27) without hydrogen coolant in the reflector-moderator materials. The results of these calculations indicate a critical mass of 28.0 lb in the spherical assembly. Further calculations were made using the same cross sections for the neutron transport theory code DTF-II (Ref. 18). In the transport theory calculations the reflector-moderator materials sometimes included hydrogen coolant and sometimes omitted it. In these cases there was an increase of $2\frac{1}{2}\%$ in K_{eff} when hydrogen coolant was removed from the reflector-moderator. The results of the transport theory calculations with hydrogen indicate a critical mass in the spherical assembly of 32.3 lb. Applying an equivalent correction to the diffusion theory results to

allow for the presence of hydrogen in the reflector-moderator raised the diffusion theory critical mass to 31.3 lb. This rather close correspondence between S4 transport theory and diffusion theory indicates that the two-dimensional results from diffusion theory can be assumed to be reasonably accurate.

Earlier, it had been indicated that a critical mass of 43. 1 lb could be achieved in a modification of the engine design of Ref. 25 which consisted of cutting the exhaust nozzle approach slot volume in half. Critical mass for the equivalent spherical configuration was 37.25 lb (see Fig. 10 of Ref. 1). By applying the same scaling factor to the present spherical calculations to estimate a two-dimensional result, the indicated critical mass for the two-dimensional counterpart of the configuration with the three modifications specified above would be 37.5 lb of U-233.

COMPARISON OF NUCLEAR LIGHT BULB AND OPEN-CYCLE ENGINE RESULTS

The lowest U-233 critical mass calculated for the nuclear light bulb engine is 38.3 lb for configuration I. The critical mass of U-233 for the most recent open-cycle engine design is 37.5 lb. Both of these configurations had no impurities in either the BeO or graphite but did have different amounts of structure, plumbing, and NbC coatings within the moderator regions.

The major differences between the two configurations are (1) the nuclear light bulb has internal moderation, and (2) thermal neutron absorption in the end walls of the nuclear light bulb engine is much greater than for the open-cycle engine. The engines are similar in that the total cavity volume of the seven units in the nuclear light bulb engine is equal to the single cavity volume of the open-cycle engine.

Preliminary diffusion theory calculations have indicated that, for equal moderator and cavity volumes, a cavity reactor with some internal moderation should require critical masses as much as 25% lower than the critical mass required in a single cavity. Comparison of axial and radial neutron flux plots in Figs. 9 and 10 reveals that there is a build up and inward flow of Group-4 neutrons from the BeO region into the fuel regions in the radial direction, while in the axial direction there appears to be aggravated absorption of thermal neutrons in the end walls causing large outward axial leakage. A comparison of absorption properties of the nuclear light bulb and open-cycle end walls can be made by calculating the thicknesses of the regions in group-4 neutron absorption mean-free-paths, $\Sigma_a \ell$. The results of this calculation indicate that $\Sigma_a \ell = 1.37 \times 10^{-2}$ for the open-cycle end walls and 4.50×10^{-1} for the nuclear light bulb end walls. Further results from Table X indicate that the radial thickness of the outer BeO and graphite regions of the nuclear light bulb engine in group-4 neutron absorption mean-free-paths is $\Sigma_a \ell = 4.91 \times 10^{-3}$, two orders of magnitude less than the end-wall value.

It is difficult to estimate how much lower the U-233 critical mass can be in the nuclear light bulb engine. The conflicting factors which affect criticality must be examined more thoroughly. First, two factors will tend to increase the critical mass calculated for configuration I, namely, (1) the inclusion of impurities in far lower concentrations than indicated in Table IX in the BeO and graphite, and (2) the effect of apparent shelf shielding when the U-233 is not distributed uniformly in the cavity regions. Conflicting with these trends will be the strong tendency to decrease critical mass by removing absorbers from the end walls and improving axial reflection.

Figure 16 shows a comparison of the integrated U-233 fission neutrons sources from the one-dimensional transport theory calculations for the open-cycle engine and the nuclear light bulb configuration C. It can be seen from these figures that

16

the hot hydrogen at the very much higher temperature and the absence of internal moderation cause more of the neutron source to be generated above 0.5 ev in the open-cycle engine than in the nuclear light bulb engine.

REFERENCES

1. Latham, T. S.: Nuclear Criticality Study of a Specific Vortex-Stabilized Gaseous Nuclear Rocket Engine. United Aircraft Research Laboratories Report E-910375-1, October 1966.

2. McLafferty, G. H., and H. E. Bauer: Studies of Specific Nuclear Light Bulb and Open-Cycle Gaseous Nuclear Rocket Engines. United Aircraft Research Laboratories Report F-910093-37, September 1967.

3. Bell, G. I.: Calculations of the Critical Mass of UF_6 as a Gaseous Core with Reflectors of D_2O, Be, and C. Los Alamos Report LA-1874, February 1955.

4. Safonov, G.: The Criticality and Some Potentialities of Cavity Reactors. Rand Corporation Research Memorandum RM-1835, July 1955.

5. Safonov, G.: Engineering Test Reactors with Large Central Irradiation Cavities. Nuclear Science and Engineering, Vol. 2, No. 4, July 1957, p. 527.

6. Ragsdale, R. G., and R. E. Hyland: Some Nuclear Calculations of U-235 D_2O Gaseous Core Cavity Reactors. NASA TN D-475, October 1961.

7. Mills, C. G.: Reflector Moderated Reactors. Nuclear Science and Engineering, Vol. 13, No. 4, August 1962, p. 301.

8. Hyland, R. E., R. G. Ragsdale, and F. J. Gunn: Two Dimensional Criticality Calculations of Gaseous-Core Cylindrical-Cavity Reactors. NASA TN D-1575, March 1963.

9. Holl, R. J., and T. F. Plunkett: Cavity Nuclear Reactors. Douglas Paper No. 1738, July 1963.

10. Hubbard, H. W., A. L. Latter, and E. A. Martinelli: Second Report on Propulsion by a Gaseous Fission Reactor. Rand Memorandum RM-3851-AEC, October 1963.

11. Butler, W. R., H. C. Chang, and J. A. Vreeband: A Transport Theory Analysis of A Gaseous Core Concept. Aerojet-General REON Report RN-TM-0190, May 1965.

12. Herwig, L. O., and T. S. Latham: Nuclear Characteristics of Large Reflector-Moderated Gaseous-Fueled Cavity Reactors Containing Hot Hydrogen. AIAA Journal, Vol. 5, No. 5, May 1967, p. 930.

13. Tumm, G. W.: U-235 Resonance Cross Sections and Gaseous Core Reactor Calculations. Plasma Research Laboratory Report No. 22, Columbia University, New York, August 1965.

REFERENCES (Contd.)

14. Eriksen, J. A., R. M. Kaufman, W. F. Osborn, E. B. Roth, J. R. Simmons, and A. H. Foderaro: Gaseous-Fueled Cavity Reactors - Criticality Calculations and Analysis. General Motors Corporation, NASA CR-487, July 1966.

15. Byers, C. C.: Private Communication. Los Alamos Scientific Laboratory, Dec. 1961.

16. Jarvis, G. A., and C. C. Byers: Critical Mass Measurements for Various Fuel Configurations in the LASL D_2O Reflected Cavity Reactor. AIAA Paper No. 65-555, AIAA Propulsion Joint Specialist Conference, June 1965.

17. Kunze, J. F., J. H. Lofthouse, G. D. Pinock, R. E. Wood, and R. E. Hyland: Cavity Reactor Critical Experiment, General Electric Report GEMP-473, October 7, 1966.

18. Engle, W. W., M. A. Boling, and B. W. Colston: DTF-II, A One-Dimensional, Multigroup Neutron Transport Program. Atomics International Report NAA-SR-10951, March 25, 1966.

19. Engle, W. W.: A Users Manual for ANISN, A One Dimensional Discrete Ordinates Transport Code with Anisotropic Scattering. Union Carbide Corporation Nuclear Division Report No. K-1693, March 30, 1967.

20. Mynatt, F. R.: A Users Manual for DOT, A Two Dimensional Discrete Ordinates Transport Code with Anisotropic Scattering. Union Carbide Corporation Nuclear Division Report K-1964 (In Publication).

21. Joanou, G. D., and J. S. Dudek: GAM-1, A Consistent P-1 Multigroup Code for the Calculation of Fast Neutron Spectra and Multigroup Constants. General Atomics Report GA-1850, June 1961.

22. Shudde, R. H., and J. Dyer: TEMPEST, A Neutron Thermalization Code. North American Aviation, September 1960.

23. Canfield, E. H., R. N. Stuart, R. P. Freis, and W. H. Collins: SOPHIST-I, An IBM 709/7090 Code which Calculates Multigroup Transfer Coefficients for Gaseous Moderators. University of California Lawrence Radiation Laboratory Report UCRL-5956, Livermore, California, October 1961.

24. Latham, T. S.: Heat Generation in Nuclear Fuel During Injection Into a Gaseous Nuclear Rocket Engine. AIAA Paper No. 66-620, AIAA Second Propulsion Joint Specialist Conference, June 1966. Also issued as United Aircraft Research Laboratories Report UAR-E57, April 1966.

REFERENCES (Contd.)

25. McLafferty, G. H., H. E. Bauer, and D. E. Sheldon: Preliminary Conceptual Design Study of a Specific Vortex-Stabilized Gaseous Nuclear Rocket Engine. United Aircraft Research Laboratories Report E-910093-29, October 1966.

26. Tobias, M. L., and T. B. Fowler: The TWENTY GRAND Program for the Numerical Solution of Few-Group Neutron Diffusion Equations in Two-Dimensions. Oak Ridge National Laboratory Report ORNL-3200, February 1962.

27. Vargofcak, D. S., W. T. Hayes, and D. W. Roeder: ULCER, A One-Dimensional Multigroup Diffusion Equation Code with Up-Scatter. Atomics International, NAA-SR-MEMO-9891, May 1964.

LIST OF SYMBOLS

$\overline{\cos\theta}$	Mean value of the cosine of the scattering angle for neutrons in the laboratory coordinate system, dimensionless
E	Neutron energy in electron volts, ev
H	Effective cylinder height, cm
K_{eff}	Effective multiplication factor, dimensionless
ℓ	Region thickness, axial or radial as noted, cm or in.
M	Mass, lb
M_c	Critical Mass, lb
T	Temperature, deg R or deg K
μ_{ij}	Probability for neutron energy transfer by scattering from neutron energy group i to j, dimensionless
$\nu\Sigma_f$	Macroscopic fission neutron production cross section, cm^{-1}
Σ_a	Macroscopic absorption cross section, cm^{-1}
Σ_{tr}	Macroscopic transport cross section, cm^{-1}
σ_s^i	Microscopic scattering cross section for neutrons in energy group i, barns
σ_{tr}^i	Microscopic transport cross section for neutrons in energy group i, barns
Φ	Neutron flux, neutrons/cm^2-sec
Φ_T	Total neutron flux integrated over entire reactor volume, neutrons/cm^2-sec

TABLE I

DIMENSIONS OF REGIONS EMPLOYED IN ONE- AND TWO-DIMENSIONAL CALCULATIONS FOR NUCLEAR LIGHT BULB ENGINE

Geometry of Regions Shown in Figs. 1, 2 and 3.
Composition of Regions Given in Tables III and IV.

Region		Radius of Region Outer Edge		Thickness of Region		Height of Region		Volume of Region		No. of Radial Mesh Points		No. of Axial Mesh Points	Temperature	
No.	Description	cm	in.	cm	in.	cm	in.	cm³	ft³	1-D	2-D		R	K
11	Inner Homogenized Unit Cell*	34.991	13.776	34.991	13.776	182.88	72.000	703,442	24.842	13	7	10	--*	--*
12	Inner BeO	53.157	20.928	18.166	7.152	182.88	72.000	920,000	32.489	5	5	10	2533	1405
13	Outer Homogenized Cells*	100.34	39.504	47.183	18.576	182.88	72.000	4,161,033	146.945	21	10	10	--*	--*
14	Outer BeO	106.223	41.820	5.883	2.316	182.88	72.000	698,180	24.656	4	3	10	2533	1405
15	Graphite Reflector	135.758	53.448	29.535	11.628	182.88	72.000	4,106,142	145.007	6	4	10	4068	2260
16	Pressure Vessel	143.378	56.448	7.620	3.000	360.17	141.80	2,406,746	84.993	5	3	33	1000	555
17		73.335	28.872	60.137	23.676	7.620	3.000	124,574	4.399	--	14	3	1000	555
18		135.758	53.448	55.596	21.888	7.620	3.000	287,293	10.146	--	11	3	1000	555
19		135.758	53.448	135.758	53.448	15.240	6.000	882,400	31.162	--	29	3	1000	555
20	Plumbing & Support Region	135.758	53.448	135.758	53.448	60.960	24.000	3,529,599	124.647	--	29	5	1000	555
21	Upper End Wall	135.758	53.448	135.758	53.448	24.892	9.800	1,441,253	50.897	--	29	4	4068	2260
22	Nozzle Approaches**	34.991	13.776	34.991	13.776	38.100	15.000	146,550	5.175	--	7	4	--**	--**
23		100.34	39.504	47.183	18.576	38.100	15.000	866,882	30.559	--	10	4	--**	--**
24	Lower End Walls	73.335	28.872	60.137	23.676	30.480	12.000	498,297	17.596	--	14	4	4068	2260
25		53.157	20.928	18.166	7.152	38.100	15.000	191,667	6.769	--	5	4	4068	2260
26		100.340	39.504	20.178	7.944	30.480	12.000	348,451	12.305	--	4	4	4068	2260
27		135.758	53.448	55.596	21.888	68.580	27.000	1,801,620	63.624	--	7	4	4068	2260
28	Nozzle Throats	13.198	5.196	13.198	5.196	30.480	15.000	16,679	0.5890	--	2	7	12000	6666
29		80.162	31.560	6.827	2.688	30.480	15.000	100,345	3.5436	--	2	7	12000	6666

* Regions 11 and 13 contain homogenized materials from detailed unit cells. See Fig. 2 and Tables II and III.

** Regions 22 and 23 contain homogenized materials from nozzle liner, propellant passages, tungsten structure, and unit cell end plug. See Fig. 4 and Ref. 2 for details of nozzle region.

TABLE II

DIMENSIONS OF REGIONS EMPLOYED IN DETAILED UNIT CELL

FOR NUCLEAR LIGHT BULB ENGINE

Geometry of Regions Shown in Fig. 2
Composition of Regions Given in Table III

Region		Radius of Region Outer Edge		Thickness of Region		Volume of Region		No. of Radial Mesh Points	Temperature	
Description	No.	cm	in	cm	in	cm³	ft³		R	K
Inner Fuel Region	1	6.858	2.700	6.858	2.700	27,022	0.943	3	63,000	35,000
Center Fuel Region	2	13.716	5.400	6.858	2.700	81,065	2.863	3	63,000	35,000
Outer Fuel Region	3	20.757	8.172	7.041	2.772	139,453	4.925	3	63,000	35,000
Hot Neon Layer	4	23.263	9.159	2.507	0.987	63,370	2.238	3	15,000	8,300
Cold Neon Layer	5	24.263	9.552	1.000	0.393	27,305	0.9643	3	2,000	1,111
Transparent Wall	6	24.751	9.745	0.490	0.193	13,742	0.4853	3	2,000	1,111
Cold Hydrogen Layer	7	25.751	10.138	1.000	0.393	29,015	1.0247	3	2,000	1,111
Hot Hydrogen Region	8	32.992	12.989	7.242	2.851	244,383	8.6303	3	12,000	6,666
Cool Hydrogen Layer	9	33.985	13.380	0.993	0.391	38,211	1.3494	3	4,000	2,222
Cell Liner *	10	34.991	13.776	1.006	0.396	39,867	1.4079	3	--*	--*

* Liner consists of beryllium metal tubes at 2000 R insulated by NbC-coated pyrolytic graphite with a surface temperature of 4068 R.

TABLE III

COMPOSITION OF REGIONS EMPLOYED IN DETAILED UNIT CELL

FOR NUCLEAR LIGHT BULB ENGINE

Dimensions of Regions Given in Table II
Geometry of Regions Shown in Fig. 2

Region			Volume Fraction									
Description	No.	U-233	Ne at 1500 R	Ne at 2000 R	SiO$_2$	H$_2$ 2000 R	H$_2$ 12,000 R	H 12,000 R	H$_2$ 4000 R	Bc	B$_4$C	Pyro C
Inner Fuel Region	1	Varied	Varied	--	--	--	--	--	--	--	--	--
Center Fuel Region	2	Varied	Varied	--	--	--	--	--	--	--	--	--
Outer Fuel Region	3	Varied	Varied	--	--	--	--	--	--	--	--	--
Hot Neon Layer	4	--	1.0	--	--	--	--	--	--	--	--	--
Cold Neon Layer	5	--	--	1.0	--	--	--	--	--	--	--	--
Transparent Wall	6	--	--	--	1.0	--	--	--	--	--	--	--
Cold Hydrogen Layer	7	--	--	--	--	1.0	--	--	--	--	--	--
Hot Hydrogen Region	8	--	--	--	--	--	0.515	0.485	--	--	--	--
Cool Hydrogen Layer	9	--	--	--	--	--	--	--	1.0	--	--	--
Cell Liner	10	--	--	--	--	0.395	--	--	--	0.070	0.021	0.514

TABLE IV

COMPOSITION OF REGIONS EMPLOYED IN ONE- AND TWO-DIMENSIONAL

CALCULATIONS FOR NUCLEAR LIGHT BULB ENGINE

Geometry of Regions Shown in Figs. 1 and 5.
Dimensions of Regions Given in Table I.

| Region | | Volume Fractions | | | | | | | | | | | |
Description	No.	BeO at 2533 R	H_2 at 2000 R	C	H_2 at 4000 R	Si-3??	I_2 at 940 R	Hf	W-Nat	B_4C	H at 12,000 R	H_2 at 12,000 R	Be
Homogenized Unit Cells *	11, 13	--	--	--	--	--	--	--	--	--	--	--	--
Inner & Outer BeO	12, 14	0.9000	0.088	--	--	--	--	--	--	--	--	--	0.012
Graphite Reflector	15	--	--	0.910	0.090	--	--	--	--	--	--	--	--
Pressure Vessel	16-19	--	--	--	--	0.950	0.050	--	--	--	--	--	--
Plumbing & Support Region	20	--	--	--	--	0.126	--	0.00006	0.004	--	--	--	--
Upper End Wall	21	--	0.415	0.514	--	0.046	--	0.00006	0.023	0.003	--	--	0.001
Lower End Wall	24-27	--	--	0.375	0.6047	--	--	--	0.010	0.0004	--	--	0.0003
Nozzle Approaches	22, 23	--	--	0.2226	--	--	--	--	0.034	--	0.3502	0.372	0.0002
Nozzle Throat	28, 29	--	--	--	--	--	--	--	--	--	0.485	0.515	--

* Volume fractions of materials in regions 11 and 13 based on fraction of total unit cell volume occupied by each of regions 1-10. See Table II for dimensions of regions in unit cell

TABLE V

SUMMARY OF NUCLEAR LIGHT BULB ENGINE CONFIGURATIONS USED FOR

ONE- AND TWO-DIMENSIONAL S4 CALCULATIONS

- Description of Configurations Given
In Tables I to IV and Fig. 1 to 3

One-Dimensional Configurations

Configuration	Effective Cylinder Height	Impurities In BeO & Graphite	U-233 Fuel Loading In Equivalent 2-D Configuration, lb	K_{eff}
A	Infinite	Yes	22.2	0.966
B	Infinite	No	22.2	1.169
C	Varied	No	Varied	Varied

Two-Dimensional Configurations

Configuration	Impurities In BeO & Graphite (See Table IX)	Poisons Due To Structure In End Walls	Hafnuim Fuel-Injection Ducts In Upper End Wall	End-Wall Moderator Configuration	U-233 Critical Mass, M_c-lb
D*	No	Yes	Yes	Reference	43.5
E	Yes	Yes	Yes	Reference	58.3
F	Yes	Yes	No	Reference	58.1
G	No	Yes	Yes	**	40.4
H	Yes	Yes	Yes	Same as G	55.4
I	No	Yes	Yes	***	38.3
J	Yes	Yes	Yes	Same as I	51.8

* Reference Configuration Of Nuclear Light Bulb Engine

** Graphite Replaced By Equal Volume of BeO In End Walls And Nozzle Approaches, Regions 21 Through 27

*** BeO Mass Doubled In Lower End Wall and Nozzle Approaches, Regions 22 Through 27

TABLE VI

DENSITIES AND WEIGHTS OF MATERIALS EMPLOYED IN

NUCLEAR LIGHT BULB CRITICALITY CALCULATIONS

Dimensions of Regions Given in Tables I and II
Composition of Regions Given in Tables III and IV
Geometry of Regions Shown in Fig. 1 to 3

Material	Atom Density, N (Atoms/cm^3) x 10^{-24}	Mass Density gm/cm^3	lb/ft^3	Total Mass In All Regions lbs
Neon, T = 15,000 R	4.417×10^{-4}	0.0148	0.9435	2.109
Neon, T = 2000 R	3.312×10^{-3}	0.111	6.926	6.676
Hydrogen, T = 12,000 R	7.26×10^{-4}	0.0012	0.0749	2.889
Hydrogen, T = 4000 R	3.30×10^{-3}	0.0058	0.3420	25.666
Hydrogen, T = 2000 R	6.60×10^{-3}	0.011	0.6864	93.36
Hydrogen, T = 540 R	1.32×10^{-2}	0.022	0.1373	8.972
NbC	4.27×10^{-2}	7.46	465.5	103.5
Be	1.23×10^{-1}	1.84	114.8	115.8
SiO$_2$	2.526×10^{-2}	2.52	157.3	76.20
BeO	7.240×10^{-2}	3.0	187.2	9,628
Pyrolytic Graphite	1.000×10^{-1}	2.0	124.8	90.311
Graphite	9.25×10^{-2}	1.84	114.8	23,383
Stainless Steel	9.01×10^{-2}	8.02	500.4	71,163
Natural Tungsten	6.09×10^{-2}	18.8	1173	5,618
Hafnium	4.45×10^{-2}	13.2	823.7	1.948

TABLE VII

NEUTRON ENERGY GROUP STRUCTURES USED IN

BOTH OPEN CYCLE AND NUCLEAR LIGHT BULB ENGINE

CRITICALITY CALCULATIONS

Neutron Energy Group	Upper Energy Limit ev	Lower Energy Limit ev	Group Number, Four-Group Structure Used For Nuclear Light Bulb Engine
1	1.0×10^7	2.865×10^6	
2	2.865×10^6	1.35×10^6	
3	1.35×10^6	8.21×10^5	1
4	8.21×10^5	3.88×10^5	
5	3.88×10^5	1.11×10^5	
6	1.11×10^5	1.50×10^4	2
7	1.50×10^4	3.35×10^3	
8	3.35×10^3	5.83×10^2	
9	5.83×10^2	1.01×10^2	
10	1.01×10^2	29.0	3
11	29.0	8.32	
12	8.32	3.06	
13	3.06	2.38	
14	2.38	1.86	
15	1.86	1.44	
16	1.44	1.125	
17	1.125	0.685	4
18	0.685	0.414	
19	0.414	0.3	
20	0.3	0.2	
21	0.2	0.1	
22	0.1	0.05	
23	0.05	0.015	
24	0.015	0.0	

TABLE VIII

COMPARISON OF RESULTS OF ONE-DIMENSIONAL 24-GROUP AND

4-GROUP S4 CALCULATIONS FOR NUCLEAR LIGHT BULB ENGINE CONFIGURATION A

- Configuration Described In Tables III to V And Fig. 3

- Impurities In BeO and Graphite

- Cylinder Height Assumed Infinite

- U-233 Fuel Loading Equivalent to 22.2 lb
  In Basic Two-Dimensional Configuration

Quantities Compared	24-Group	4-Group
Effective Multiplication Factor, K_{eff}	0.96626	0.96640
Peak Power/Average Power	1.2992	1.2840
Fuel Region Absorption/Fission	1.4235	1.4226
Neutron Absorption by Following Regions		
Fuel & Hydrogen	0.56798	0.56806
Moderators	0.21076	0.21052
Tungsten Plumbing & Pressure Vessel	0.199370	0.19832
Net Neutron Leakage in Following Regions		
Fuel & Hydrogen	0.43673	0.43110
Moderators	-0.21314	-0.21060
Tungsten Plumbing & Pressure Vessel	-0.19940	-0.19821
Neutron Flux for Group 4 in Following Regions		
(0 - 8.32 ev)		
Fuel & Hydrogen	64.659	66.768
Moderators	14.382	13.899
Tungsten Plumbing & Pressure Vessel	0.11893	0.09936
Neutron Flux for Group 3 in Following Regions		
$(8.32 - 3.35 \times 10^3 \text{ ev})$		
Fuel & Hydrogen	51.046	51.792
Moderators	26.506	26.092
Tungsten Plumbing & Pressure Vessel	0.32923	0.30891
Neutron Flux for Group 2 in Following Regions		
$(3.35 \times 10^3 - 3.88 \times 10^6 \text{ ev})$		
Fuel & Hydrogen	50.710	51.257
Moderators	31.672	31.084
Tungsten Plumbing & Pressure Vessel	0.5557	0.53846
Neutron Flux for Group 1 in Following Regions		
$(3.88 \times 10^6 - 1.0 \times 10^7 \text{ ev})$		
Fuel & Hydrogen	326.78	326.63
Moderators	242.66	243.14
Tungsten Plumbing & Pressure Vessel	2.6466	2.6232
Total Neutron Flux in Following Regions		
$(0 - 1.0 \times 10^7 \text{ ev})$		
Fuel & Hydrogen	493.20	496.45
Moderators	315.22	314.22
Tungsten Plumbing & Pressure Vessel	3.6505	3.5700
Fission Neutron Production Fraction in Fuel Region		
Center Fuel	0.17838	0.17761
Outer Fuel	0.78791	0.78879

TABLE IX

IMPURITY SPECIFICATIONS FOR
BERYLLIUM OXIDE AND GRAPHITE

- BeO Impurity Specifications Taken From
  CANEL Specification CS-2040A of
  April 29, 1959

- Graphite Impurity Specification Obtained
  From Los Alamos Scientific Laboratory,
  Private Communications

Impurity	BeO	C	Impurity	BeO	C
	ppm			ppm	
Li	1	1	St	-	5
Be	-	1	Zr	-	10
B	3	1	Nb	-	10
Na	50	10	Mo	-	10
Mg	50	1	Cd	2	1
Al	100	3	Sn	-	3
Si	20	30	Ba	-	5
K	-	15	Hf	-	30
Ca	50	3	Ta	-	30
Ti	-	5	W	-	30
V	-	3	Pb	-	3
Mn	10	1	Bi	-	3
Fe	20	3	Cr	10	-
Ni	20	3	U	20	-
Cu	5	3	Co	5	-
Zn	-	15			

TABLE X

SUMMARY OF ABSORPTION CHARACTERISTICS IN MODERATOR AND CELL REGIONS

FOR TWO-DIMENSIONAL NUCLEAR LIGHT BULB CONFIGURATIONS

- Description Of Configurations Given In Tables I to V And Fig. 1.

Description	No.	Thickness, ℓ - cm	Configuration (See Table V)	Impurities In BeO And Graphite	Region Temperature, R		Macroscopic Absorption Cross-Section In Region, ℓ, Σ_a - cm^{-1}	Region Thickness In Absorption Mean-Free-Paths, $\Sigma_a \ell$
Center Fuel	11	34.991	I	No	---	---	6.334×10^{-5}	8.545×10^{-3}
Inner BeO	12	18.166	E, F, H, J	Yes	1255	1445	1.215×10^{-3}	2.207×10^{-2}
Inner BeO	12	18.166	D, G, I	No	2533	1445	2.791×10^{-4}	5.070×10^{-3}
Outer Fuel	13	47.183	I	No	---	---	2.567×10^{-5}	1.211×10^{-3}
Outer BeO	14	5.883	E, F, H, J	Yes	2533	1445	1.151×10^{-2}	6.77×10^{-2}
Outer BeO	14	5.883	D, G, I	No	2533	1445	2.661×10^{-4}	1.555×10^{-3}
Graphite	15	29.535	E, F, H, J	Yes	4068	2260	5.710×10^{-4}	1.636×10^{-2}
Graphite	15	29.535	D, G, I	No	4068	2260	1.131×10^{-4}	3.340×10^{-3}
Pressure Vessel	16-19	7.620	D-J	--	1000	555	7.366×10^{-2}	5.613×10^{-1}
Upper End Wall	21	24.892	E	Yes	4068	2260	1.145×10^{-2}	2.859×10^{-1}
Upper End Wall	21	24.892	D	No	4068	2260	1.100×10^{-2}	2.738×10^{-1}
Upper End Wall	21	24.892	F	Yes	4068	2260	1.099×10^{-2}	2.736×10^{-1}
Upper End Wall	21	24.892	H	Yes	2533	1445	1.176×10^{-2}	2.927×10^{-1}
Upper End Wall	21	24.892	G	No	2533	1445	1.109×10^{-2}	2.761×10^{-1}
Lower End Wall**	25	38.100	E, F	Yes	4068	2260	6.785×10^{-3}	2.585×10^{-1}
Lower End Wall	25	38.100	D	No	4068	2260	6.500×10^{-3}	2.477×10^{-1}
Lower End Wall	25	38.100	H	Yes	2533	1445	6.777×10^{-3}	2.618×10^{-1}
Lower End Wall	25	38.100	G	No	2533	1445	6.957×10^{-3}	2.685×10^{-1}
Lower End wall	25	38.100	J	Yes	2533	1445	7.239×10^{-3}	2.755×10^{-1}
Lower End Wall	25	38.100	I	No	2533	1445	6.534×10^{-3}	2.189×10^{-1}
Nozzle Approaches	22, 23	38.100	E, F	Yes	---	---	1.435×10^{-2}	5.519×10^{-1}
Nozzle Approaches	22, 23	38.100	D	No	---	---	1.444×10^{-2}	4.802×10^{-1}
Nozzle Approaches	22, 23	38.100	H	Yes	---	---	1.447×10^{-2}	5.787×10^{-1}
Nozzle Approaches	22, 23	38.100	G	No	---	---	1.448×10^{-2}	1.451×10^{-1}
Nozzle Approaches	22, 23	38.100	J	Yes	---	---	1.500×10^{-2}	5.557×10^{-1}
Nozzle Approaches	22, 23	38.100	I	No	---	---	1.451×10^{-2}	5.528×10^{-1}
Nozzle Throats	28, 29	30.480	D-J	--	10000	6666	3.597×10^{-3}	2.924×10^{-1}
Plumbing & Support	20	60.960	D, E, G-J	--	1000	555	2.848×10^{-3}	1.774×10^{-1}
Plumbing & Support	20	60.960	F	--	1000	595	0.571×10^{-3}	1.145×10^{-1}

* ℓ = Radial thickness for regions 11-19, axial thickness for regions 20-49

** Same composition in Region 25 as in Region 24, 26, and 27

TABLE XI

NEUTRON FLUX ABOVE 0.111 Mev IN TRANSPARENT WALL REGION

OF NUCLEAR LIGHT BULB ENGINE CONFIGURATION C

- Description Of Configuration Given In
  Tables I To V And Fig. 3

- Fluxes Taken From Center Unit Cell Fuel
  Region Of One-Dimensional, 24-Group,
  S4 Calculation

- No Impurities In BeO And Graphite

- Effective Cylinder Height = 268.5 cm

- Ratio Of Center Fuel Region Flux To Outer
  Fuel Region Flux Per Unit Cell = 1.477

Energy Range Mev	Neutron Flux Normalized To Production In Fuel Regions Of 1 Neutron/Sec	Neutron Flux Normalized To Power Level Of 4600 Mw
$2.865 \rightarrow 10.0$	2.692×10^{-6}	9.635×10^{14}
$1.350 \rightarrow 2.865$	5.047×10^{-6}	1.807×10^{15}
$0.821 \rightarrow 1.350$	3.495×10^{-6}	1.251×10^{15}
$0.388 \rightarrow 0.821$	3.588×10^{-6}	1.284×10^{15}
$0.111 \rightarrow 0.388$	4.540×10^{-6}	1.625×10^{15}

TABLE XII

VARIATION OF EFFECTIVE MULTIPLICATION FACTOR AND U-233 CRITICAL MASS
WITH MATERIAL TEMPERATURES FROM ONE-DIMENSIONAL 24-GROUP, S4
CALCULATIONS FOR NUCLEAR LIGHT BULB ENGINE CONFIGURATION C

- Configuration Described In Tables I To V
    And Fig. 3

- No Impurities In BeO And Graphite

- Effective Cylinder Height = 268.5 cm

- Gas Densities Constant For All Temperatures

Variation in Material Temperature	Effective Multiplication Factor for Constant U-233 Mass of 38.3 lb	Critical Mass, M_c-lb
None, C = 4068 R BeO = 2533 R Hot Hydrogen, Reg 8 = 12,000 R	1.0000	38.3
C = 4475 R BeO = 2781 R	0.996	38.6
C = 3661 R BeO = 2277 R	0.995	39.0
C = 2034 R BeO = 1265 R Hot Hydrogen, Reg 8 = 8000 R	0.846	59.6
All Regions 540 R	1.087	27.6

TABLE XIII

SUMMARY OF ABSORPTION CHARACTERISTICS IN MODERATOR AND CELL REGIONS OF

NUCLEAR LIGHT BULB ENGINE FOR VARIOUS MATERIAL TEMPERATURES

- Configuration Described In Tables I To V And Fig. 3

- No Impurities In BeO And Graphite

- Effective Cylinder Height = 268.5 cm

- Gas Densities Constant For All Temperatures

- K_{eff} For Constant U-233 Mass And M_c From 1-D Calculations Given In Table XII

Region Description	No.	Radial Thickness, ℓ-cm	Region Temperature R	Region Temperature K	Macroscopic Absorption Cross Section In Group 4, Σ_a -cm^{-1}	Region Thickness In Absorption Mean-Free-Paths, $\Sigma_a \ell$
Center Fuel*	11	34.991	----	----	2.551×10^{-3}	8.926×10^{-2}
Center Fuel**	11	34.991	----	----	2.723×10^{-3}	9.528×10^{-2}
Center Fuel***	11	34.991	----	----	3.943×10^{-3}	1.380×10^{-1}
Inner BeO	12	18.166	2533	1405	2.791×10^{-4}	5.070×10^{-3}
Inner BeO	12	18.166	2781	1545	2.700×10^{-4}	4.905×10^{-3}
Inner BeO	12	18.166	2277	1265	2.862×10^{-4}	5.199×10^{-3}
Inner BeO	12	18.166	1265	702.5	3.498×10^{-4}	6.345×10^{-3}
Inner BeO	12	18.166	540	300	4.241×10^{-4}	7.704×10^{-3}
Outer Fuel*	13	47.183	----	----	2.567×10^{-3}	1.211×10^{-1}
Outer Fuel**	13	47.183	----	----	2.727×10^{-3}	1.287×10^{-1}
Outer Fuel***	13	47.183	----	----	4.007×10^{-3}	1.891×10^{-1}
Outer BeO	14	5.883	2533	1405	2.661×10^{-4}	1.565×10^{-3}
Outer BeO	14	5.883	2781	1545	2.596×10^{-4}	1.527×10^{-3}
Outer BeO	14	5.883	2277	1265	2.729×10^{-4}	1.605×10^{-3}
Outer BeO	14	5.883	1265	702.5	3.342×10^{-4}	1.966×10^{-3}
Outer BeO	14	5.883	540	300	4.326×10^{-4}	2.545×10^{-3}
Graphite	15	29.535	4068	2260	1.134×10^{-4}	3.340×10^{-3}
Graphite	15	29.535	4475	2486	1.111×10^{-4}	3.281×10^{-3}
Graphite	15	29.535	3661	2034	1.176×10^{-4}	3.485×10^{-3}
Graphite	15	29.535	2034	1130	1.470×10^{-4}	4.342×10^{-3}
Graphite	15	29.535	540	300	2.082×10^{-4}	6.149×10^{-3}

* Region 11 And 13 Composition As Specified In Tables III
** Hydrogen At 12,000 R Replaced By Hydrogen At 8000 R In Regions 11 And 13, BeO At 1265 R, C At 2034 R
*** All Hydrogen At 540 R, BeO And C At 540 R

TABLE XIV

DIMENSIONS OF REGIONS EMPLOYED IN ONE-DIMENSIONAL CALCULATIONS

FOR OPEN-CYCLE ENGINE

Geometry Shown in Fig. 13
Composition of Regions Given in Table XV

Region		Radius of Region Outer Edge		Thickness of Region		Volume of Region		No. of Radial Mesh Points In Each Region	Temperature of Region	
Description	No.	cm	in.	cm	in.	cm³	ft³		R	K
Inner Fuel Region	1	50.099	19.274	50.099	19.274	526,693	18.600	8	100,000	55,555
Center Fuel Region	2	63.101	24.843	13.002	5.119	525,702	18.565	4	100,000	55,555
Outer Fuel Region	3	72.919	28.708	9.818	3.865	524,003	18.505	3	100,000	55,555
Hot Hydrogen Layer	4	86.360	34.000	17.780	7.000	1,121,347	34.600	3	100,000	55,555
Cool Hydrogen Layer	5	91.440	36.000	5.080	2.000	504,634	17.821	3	5,400	3,000
Inner Liner	6	94.563	37.230	3.123	1.230	339,576	12.00	5	1,200	667
Beryllium Oxide	7	104.851	41.280	10.287	4.050	1,286,264	45.424	3	2,533	1,405
Graphite	8	140.920	55.480	36.068	14.200	6,893,330	243.436	5	4,068	2,260
Plumbing & Heat Exchanger Region	9	167.842	66.080	26.924	10.600	8,084,082	285.483	8	1,000	555
Steel Pressure Vessel	10	193.242	76.080	25.400	10.000	8,973,752	316.905	7	1,000	555

TABLE XII

COMPOSITION OF REGIONS EMPLOYED IN ONE-DIMENSIONAL CALCULATIONS FOR OPEN-CYCLE ENGINE

Dimensions of Regions Given in Table XI

Region			Volume Fractions												
Description	No.	Nuclear Fuel	Hot Hydrogen	Cool Hydrogen	H_2 at 2000 R	H_2 at 4000 R	Beryllium	BeO	Pyrolytic Graphite	W-Nat	W-184	Graphite	?	Steel
Inner Fuel Region	1	Varied	--	--	--	--	--	--	--	--	--	--	--	--
Center Fuel Region	2	Varied	Varied	--	--	--	--	--	--	--	--	--	--	--
Outer Fuel Region	3	Varied	Varied	--	--	--	--	--	--	--	--	--	--	--
Hot Hydrogen Layer	4	--	1.0	--	--	--	--	--	--	--	--	--	--	--
Cool Hydrogen Layer	5	--	--	1.0	--	--	--	--	--	--	--	--	--	--
Inner Liner	6	--	--	--	0.0946	--	0.256	--	0.412	--	0.0023	--	0.5265	--
Beryllium Oxide	7	--	--	--	0.138	--	--	0.844	0.00803	--	--	--	--	--
Graphite	8	--	--	--	--	0.123	--	--	--	--	--	0.872	0.0005	--
Plumbing & Heat Exchanger Region	9	--	--	--	0.924	--	0.0267	--	0.0167	0.0324	--	--	--	--
Steel Pressure Vessel	10	--	--	--	--	--	--	--	--	--	--	--	--	0.900

FIG. 1

BASIC CYLINDRICAL GEOMETRY USED IN TWO-DIMENSIONAL
CALCULATIONS FOR NUCLEAR LIGHT BULB ENGINE

CONFIGURATION SYMMETRICAL ABOUT AXIAL CENTERLINE

CIRCLED NUMBERS INDICATE REGIONS DESCRIBED IN TABLES I TO IV

DOTTED LINES INDICATE ADJACENT REGIONS CONTAIN IDENTICAL MATERIALS
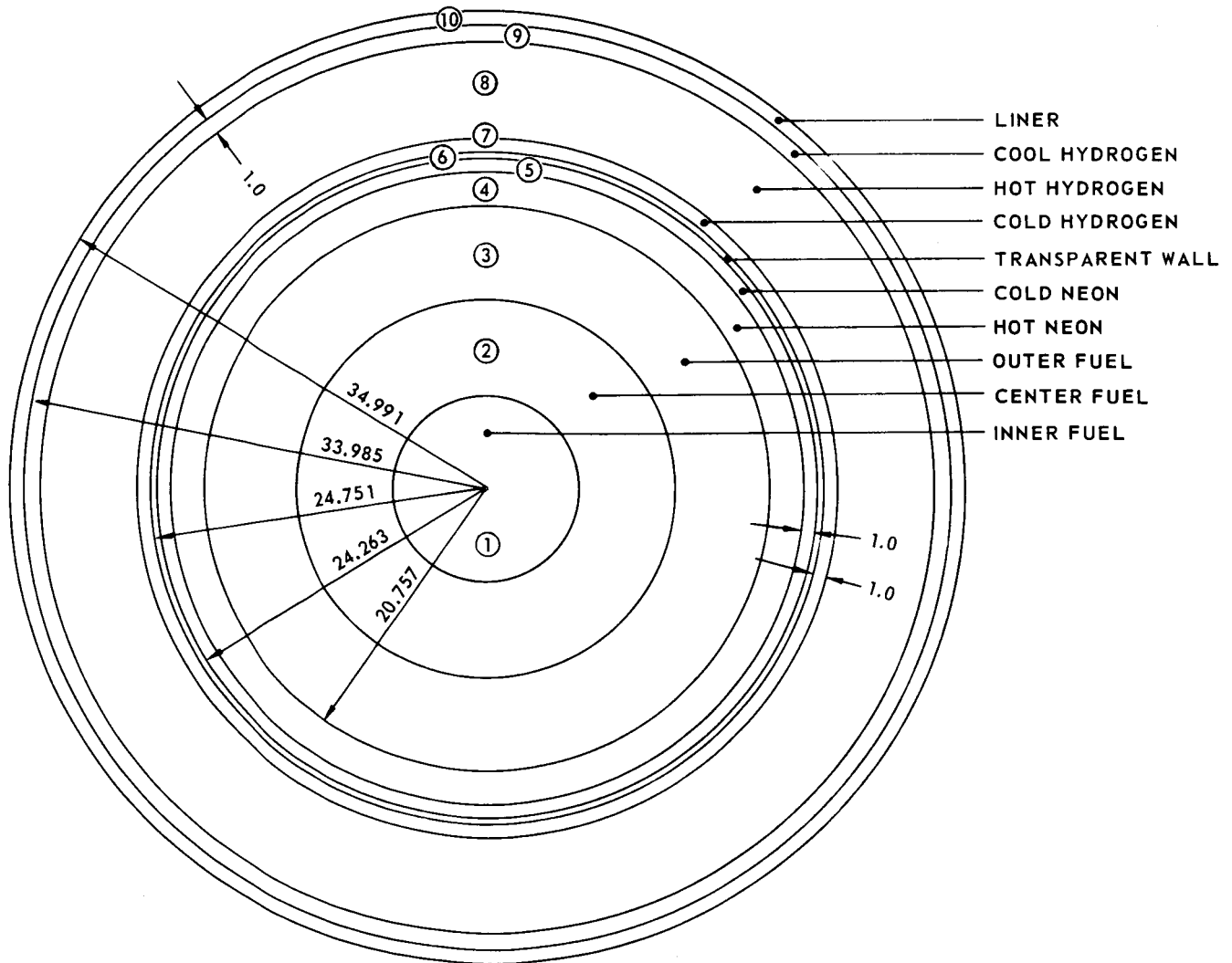
ALL DIMENSIONS IN CM
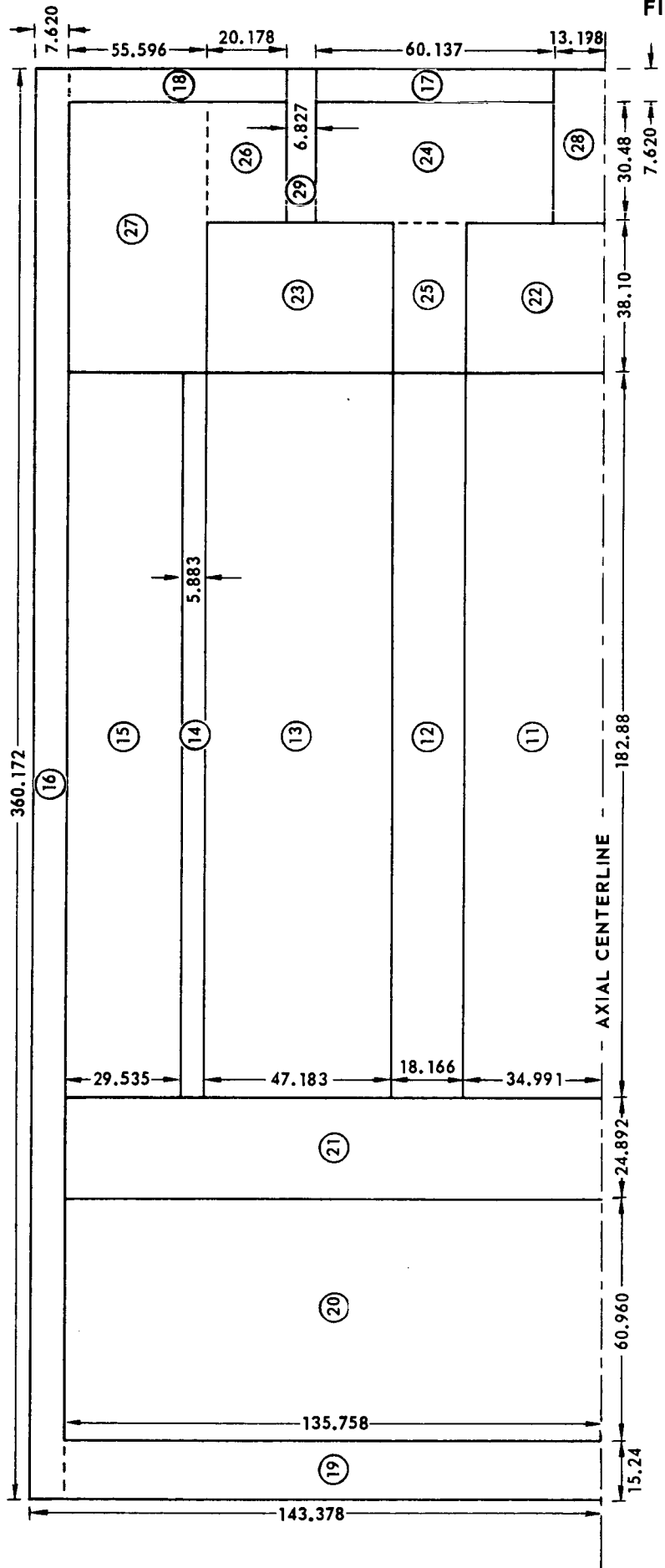
CROSS SECTION OF DETAILED UNIT CELL FOR NUCLEAR LIGHT BULB ENGINE

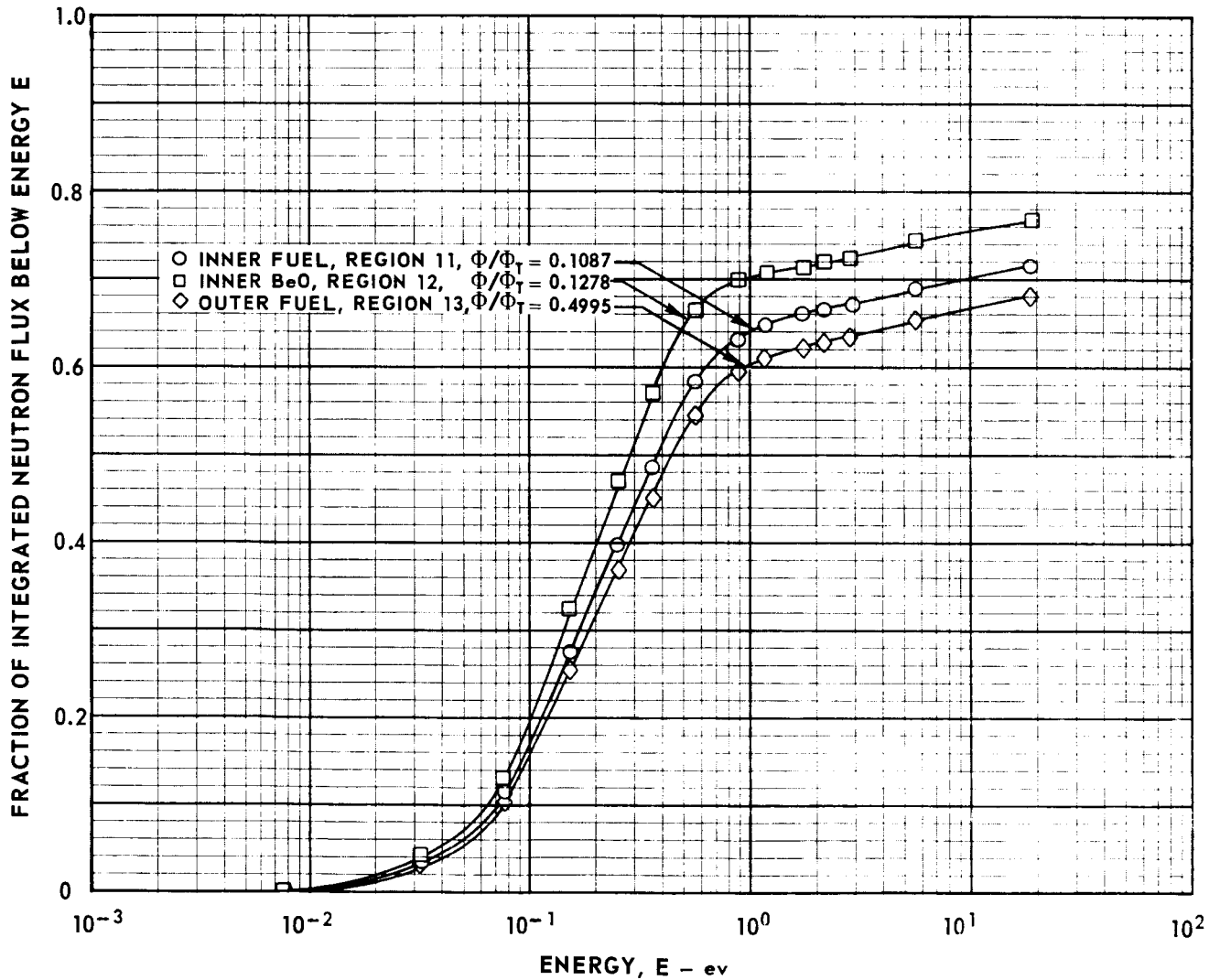CIRCLED NUMBERS INDICATE REGIONS DESCRIBED IN TABLES II AND III

ALL DIMENSIONS IN CM

LINER
COOL HYDROGEN
HOT HYDROGEN
COLD HYDROGEN
TRANSPARENT WALL
COLD NEON
HOT NEON
OUTER FUEL
CENTER FUEL
INNER FUEL

34.991
33.985
24.751
24.263
20.757
1.0
1.0
1.0

CROSS SECTION AT AXIAL MID-PLANE OF BASIC CYLINDRICAL
GEOMETRY USED FOR ONE-DIMENSIONAL CALCULATIONS
FOR NUCLEAR LIGHT BULB ENGINE

CIRCLED NUMBERS INDICATE REGIONS DESCRIBED IN TABLES I TO IV

DOTTED LINES INDICATE ADJACENT REGIONS HOMOGENIZED

ALL DIMENSIONS IN CM
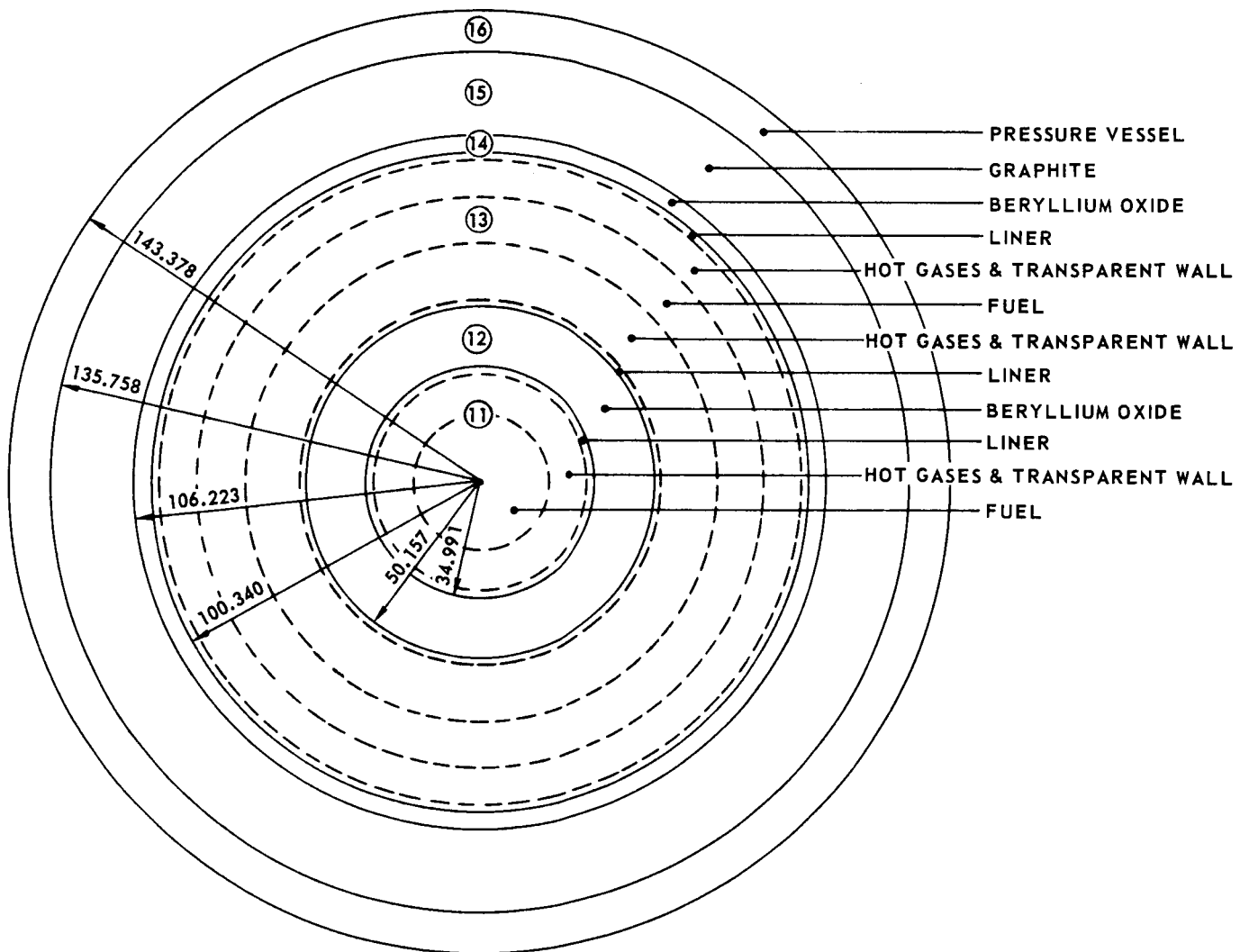
FIG. 4

INTEGRATED FLUXES FROM ONE-DIMENSIONAL, 24-GROUP,
S4 CALCULATIONS FOR NUCLEAR LIGHT BULB ENGINE CONFIGURATION A

CONFIGURATION A DESCRIPTION GIVEN IN TABLES I TO V AND FIG. 3

CYLINDER HEIGHT ASSUMED INFINITE

U-233 FUEL LOADING EQUIVALENT TO 22.2 LB IN TWO-DIMENSIONAL CONFIGURATION

FRACTION OF INTEGRATED NEUTRON FLUX BELOW ENERGY E

ENERGY, E - ev

O INNER FUEL, REGION 11, $\Phi/\Phi_T = 0.1087$
□ INNER BeO, REGION 12, $\Phi/\Phi_T = 0.1278$
◇ OUTER FUEL, REGION 13, $\Phi/\Phi_T = 0.4995$

RESULTS OF TWO–DIMENSIONAL, 4–GROUP, S4 CALCULATIONS FOR NUCLEAR LIGHT BULB ENGINE WITH NO IMPURITIES IN BeO AND GRAPHITE

DESCRIPTION OF CONFIGURATIONS GIVEN IN TABLES I TO V AND FIG. 1

EIGENVALUE CONVERGENCE ≤ 0.0005

SYMBOL	CONFIGURATION (SEE TABLE V)	CHANGES FROM REFERENCE CONFIGURATION	M_c –LB	$(\Delta K/K)/(\Delta M/M_c)$
O	D	NONE	43.5	—
◇	G	GRAPHITE REPLACED BY EQUAL VOLUME OF BeO IN END WALLS AND NOZZLE APPROACHES, REGIONS 21 THROUGH 27	40.4	—
□	I	BeO MASS DOUBLED IN LOWER END WALL AND NOZZLE APPROACHES, REGIONS 22 THROUGH 27	38.3	0.563
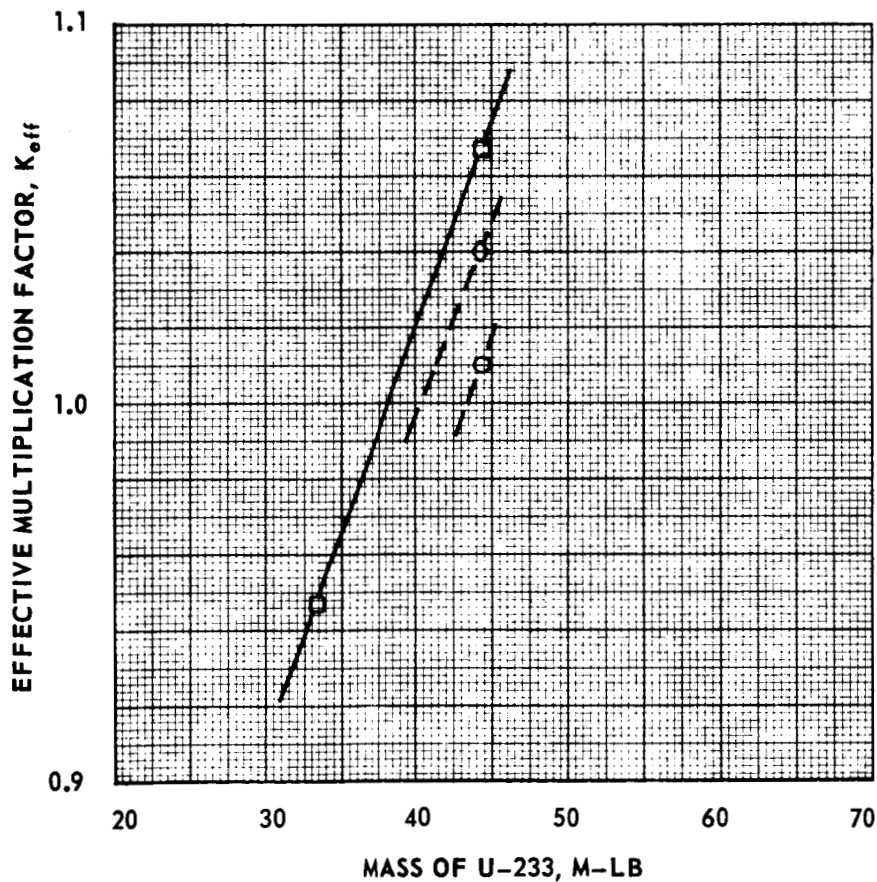
RESULTS OF TWO-DIMENSIONAL, 4-GROUP, S4 CALCULATIONS FOR NUCLEAR LIGHT BULB ENGINE WITH IMPURITIES IN BeO AND GRAPHITE

DESCRIPTION OF CONFIGURATIONS GIVEN IN TABLES I TO V AND FIG. 1

IMPURITIES IN BeO AND GRAPHITE LISTED IN TABLE IX

EIGENVALUE CONVERGENCE ≤ 0.0005

SYMBOL	CONFIGURATION (SEE TABLE V)	CHANGES FROM REF. CONFIGURATION OTHER THAN ADDITION OF IMPURITIES	M_c −LB	$(\Delta K/K)/(\Delta M/M_c)$
O	E	NONE	58.3	0.389
△	F	HAFNIUM FUEL INJECTION DUCTS REMOVED FROM REGIONS 20 & 21	58.1	−
◇	H	GRAPHITE REPLACED BY EQUAL VOLUME OF BeO IN END WALLS AND NOZZLE APPROACHES, REGIONS 21 THROUGH 27.	55.4	−
□	J	BeO MASS DOUBLED IN LOWER END WALL AND NOZZLE APPROACHES, REGIONS 22 THROUGH 27	51.8	0.588
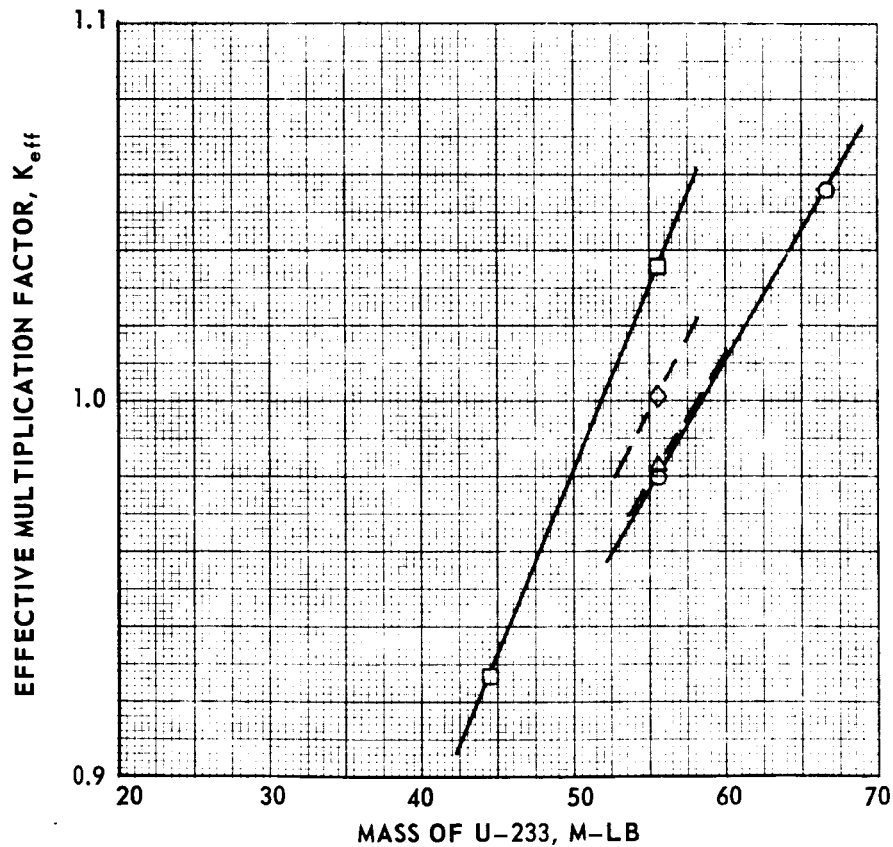
VARIATION OF EFFECTIVE MULTIPLICATION FACTOR WITH EFFECTIVE CYLINDER HEIGHT FOR ONE-DIMENSIONAL, 24-GROUP, S4 CRITICALITY CALCULATIONS USING CONSTANT U-233 MASS LOADING IN NUCLEAR LIGHT BULB ENGINE CONFIGURATION C

M_c = 38.3 FROM RESULTS OF 2-D CALCULATIONS FOR CONFIGURATION I (SEE TABLE V)

DESCRIPTION OF 1-D CONFIGURATION GIVEN IN TABLES I TO V AND FIG. 3

FOR K_{eff} = 1.0, H = 268.5 CM

EFFECTIVE MULTIPLICATION FACTOR, K_{eff}
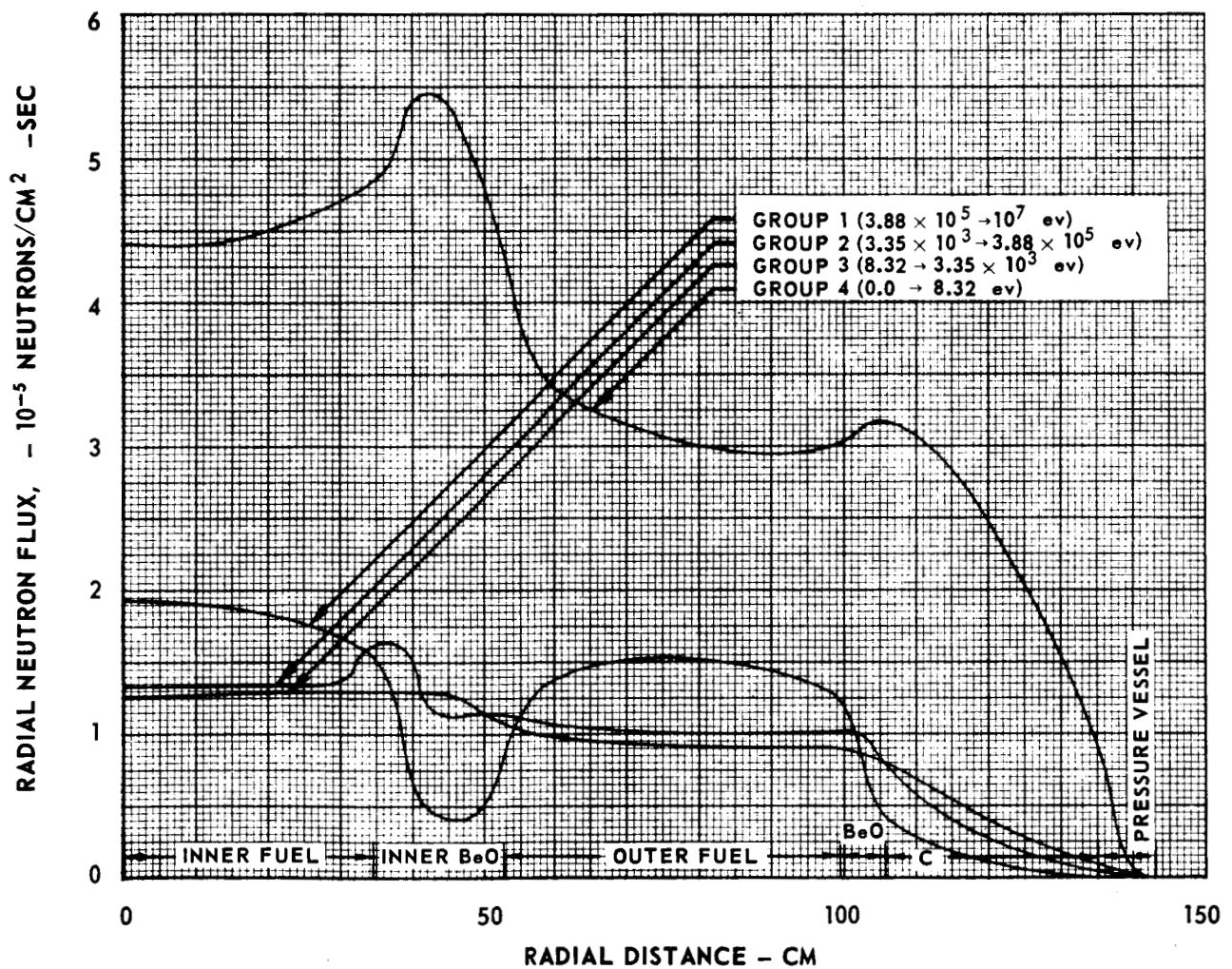
EFFECTIVE CYLINDER HEIGHT, H-CM

FIG. 8
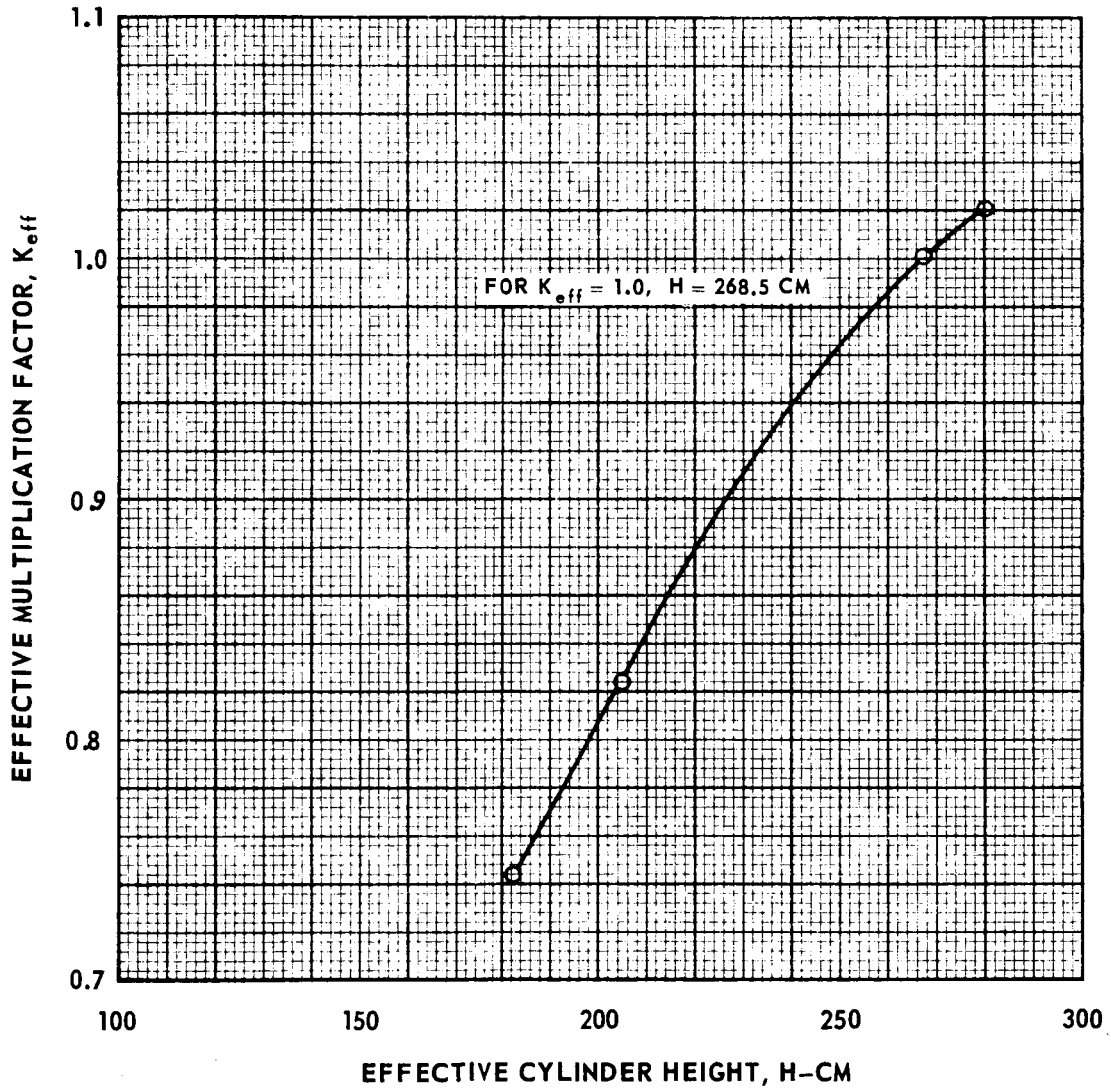
COMPARISON OF MID—PLANE RADIAL NEUTRON FLUX PLOTS FROM ONE—AND TWO—DIMENSIONAL, 4—GROUP, S4 CALCULATIONS FOR NUCLEAR LIGHT BULB ENGINE

CONFIGURATIONS C AND I

M_c = 38.3 LB FOR BOTH 1—D AND 2—D CALCULATIONS

1—D CONFIGURATION C DESCRIBED IN TABLES I TO V AND FIG. 3 WITH EFFECTIVE CYLINDER HEIGHT OF 268.5 CM

2—D CONFIGURATION I DESCRIBED IN TABLES I TO V AND FIG. 1

2—D FLUXES NORMALIZED SUCH THAT NEUTRON PRODUCTION IN FUEL REGIONS = 1 NEUTRON/SEC, 1—D FLUXES NORMALIZED SUCH THAT MID—POINT GROUP—4 FLUX EQUALED THAT FROM 2—D CALCULATION
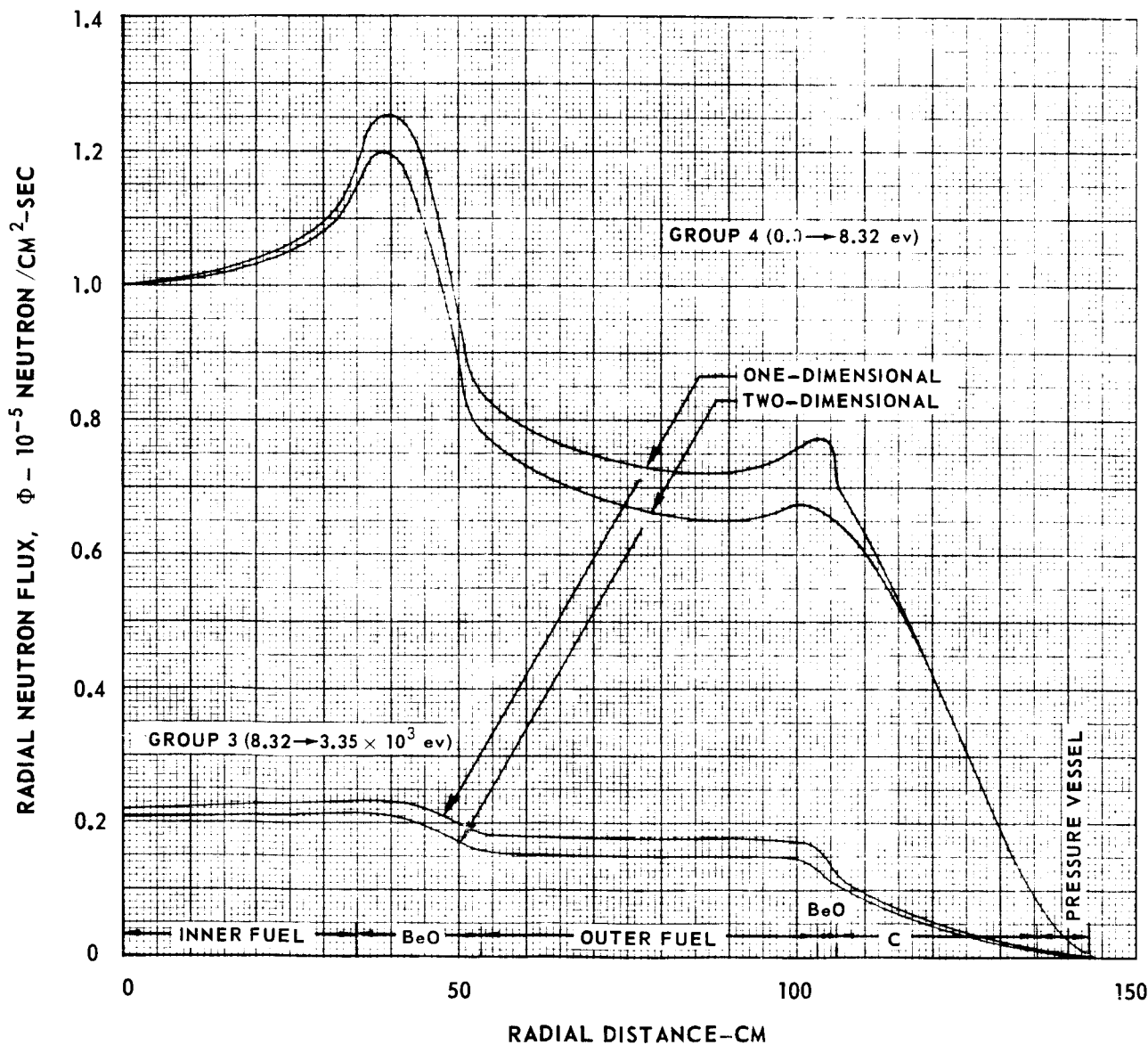
MID-PLANE RADIAL NEUTRON FLUX PLOTS FROM TWO-DIMENSIONAL,
4-GROUP, S4 CALCULATIONS FOR NUCLEAR LIGHT BULB ENGINE CONFIGURATION H

M_c = 55.4 LB FOR CONFIGURATION H (SEE TABLE V) WITH IMPURITIES IN BeO AND GRAPHITE

DESCRIPTION OF CONFIGURATION H GIVEN IN TABLES I TO V

FLUXES NORMALIZED SUCH THAT NEUTRON PRODUCTION IN FUEL REGIONS = 1 NEUTRON/SEC

GROUP 1 ($3.88 \times 10^5 \rightarrow 10^7$ ev)
GROUP 2 ($3.35 \times 10^3 \rightarrow 3.88 \times 10^5$ ev)
GROUP 3 ($8.32 \rightarrow 3.35 \times 10^3$ ev)
GROUP 4 ($0.0 \rightarrow 8.32$ ev)

RADIAL NEUTRON FLUX, $- 10^{-5}$ NEUTRONS/CM^2 -SEC

RADIAL DISTANCE - CM

INNER FUEL   INNER BeO   OUTER FUEL   BeO   C   PRESSURE VESSEL

CENTERLINE AXIAL NEUTRON FLUX PLOTS FROM TWO-DIMENSIONAL,
4-GROUP, S4 CALCULATIONS FOR NUCLEAR LIGHT BULB ENGINE CONFIGURATION H

M_C = 55.4 LB FOR CONFIGURATION H (SEE TABLE V) WITH IMPURITIES IN BeO AND GRAPHITE

DESCRIPTION OF CONFIGURATION H GIVEN IN TABLES I TO V AND FIG. 1

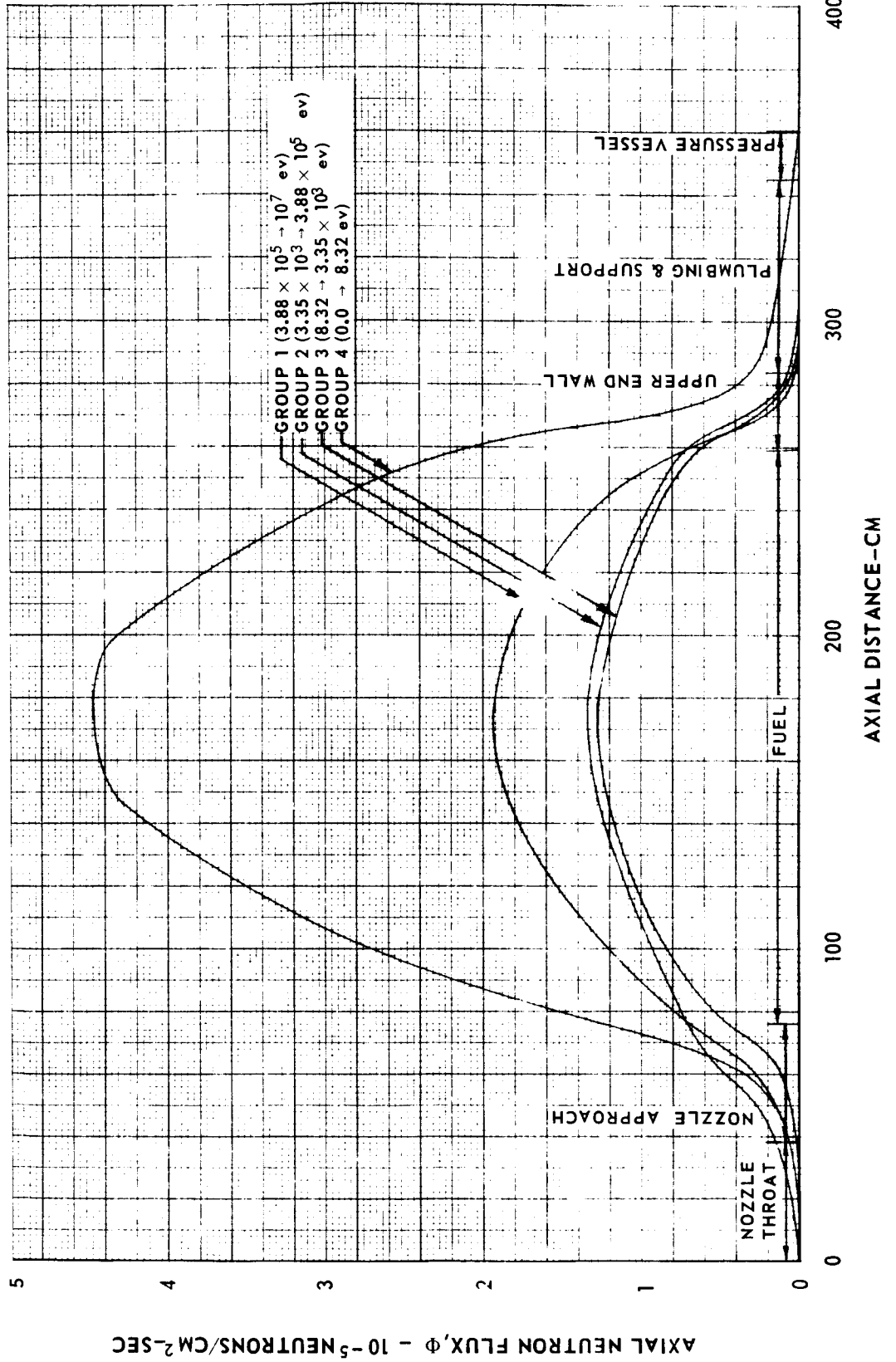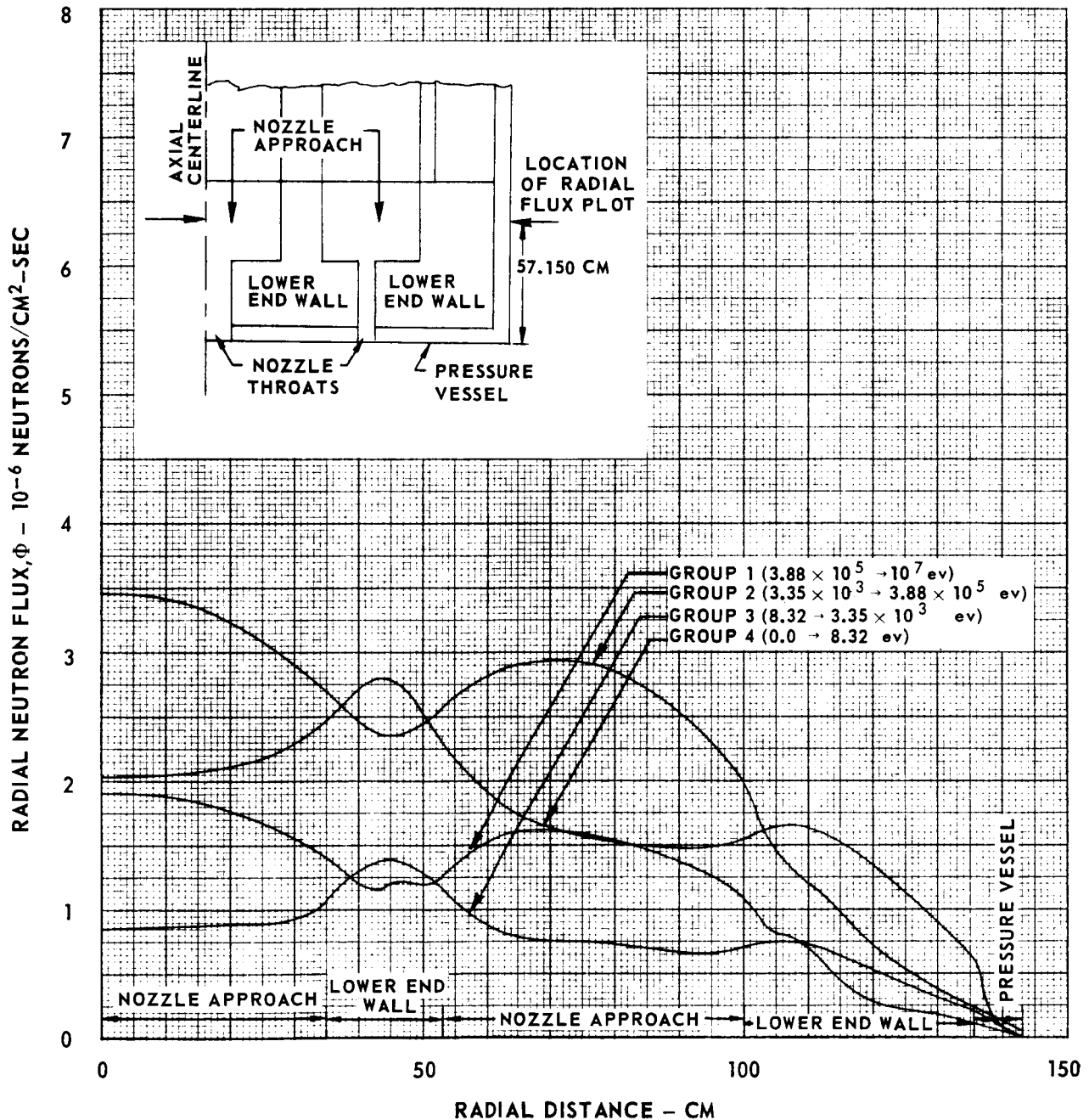FLUXES NORMALIZED SUCH THAT NEUTRON PRODUCTION IN FUEL REGIONS = 1 NEUTRON/SEC

RADIAL NEUTRON FLUX PLOTS THROUGH AXIAL MID-PLANE
OF LOWER END WALL AND EXHAUST NOZZLE APPROACHES
FROM TWO-DIMENSIONAL, 4-GROUP, S4 CALCULATIONS FOR
NUCLEAR LIGHT BULB ENGINE CONFIGURATION H

M_c = 55.4 LB FOR CONFIGURATION H (SEE TABLE V) WITH IMPURITIES IN BeO AND GRAPHITE

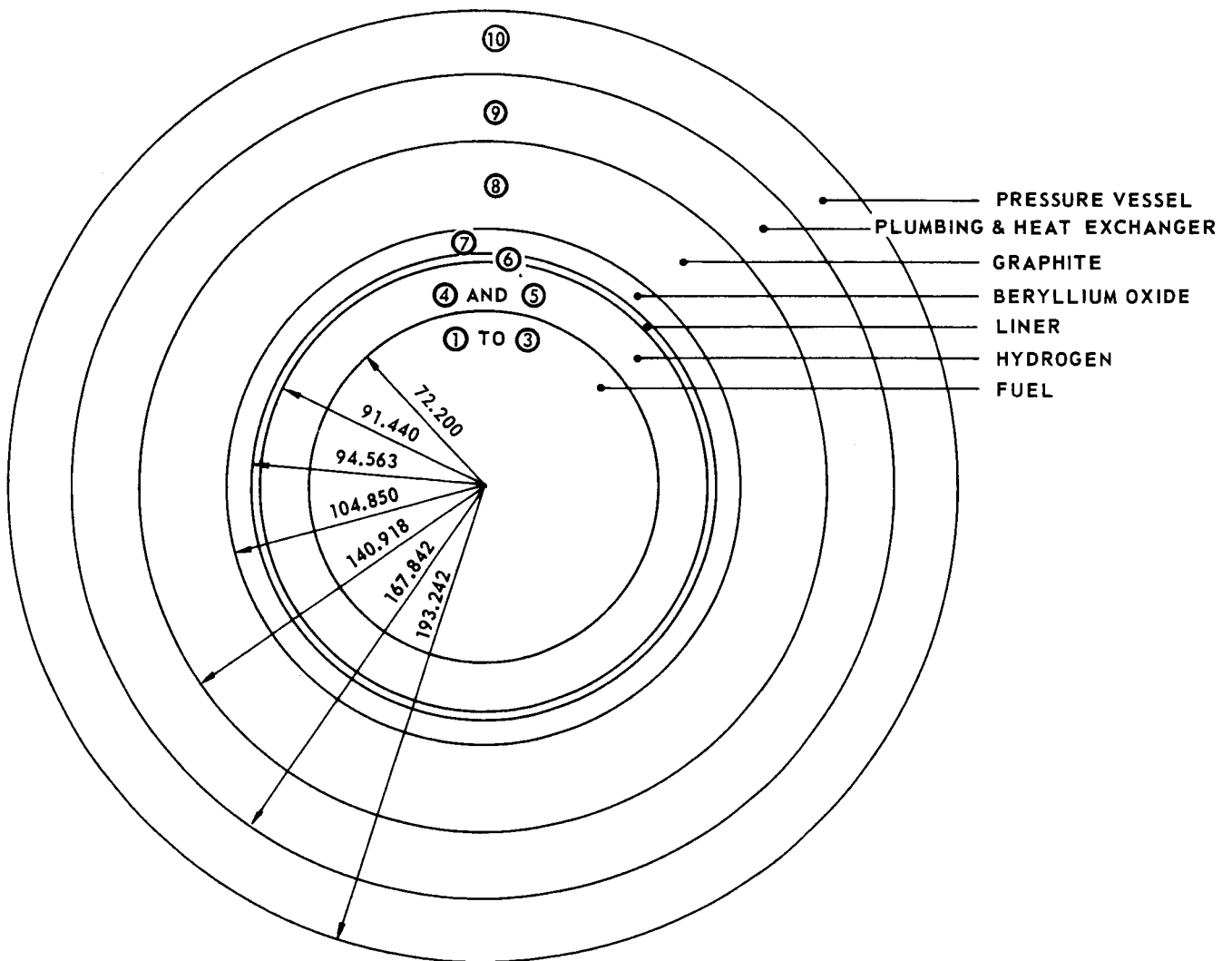DESCRIPTION OF CONFIGURATION H GIVEN IN TABLES I TO V AND FIG. 1

FLUXES NORMALIZED SUCH THAT NEUTRON PRODUCTION IN FUEL REGIONS = 1 NEUTRON/SEC

FIG. 12

RADIAL NEUTRON FLUX PLOTS THROUGH AXIAL MID-PLANE
OF NOZZLE THROAT REGIONS FROM TWO-DIMENSIONAL,
4-GROUP, S4 CALCULATIONS FOR NUCLEAR LIGHT BULB ENGINE CONFIGURATION H

M_c = 55.4 LB FOR CONFIGURATION H(SEE TABLE V) WITH IMPURITIES IN BeO AND GRAPHITE

DESCRIPTION OF CONFIGURATION H GIVEN IN TABLES I TO V AND FIG. 1

FLUXES NORMALIZED SUCH THAT NEUTRON PRODUCTION IN FUEL REGIONS = 1 NEUTRON/SEC
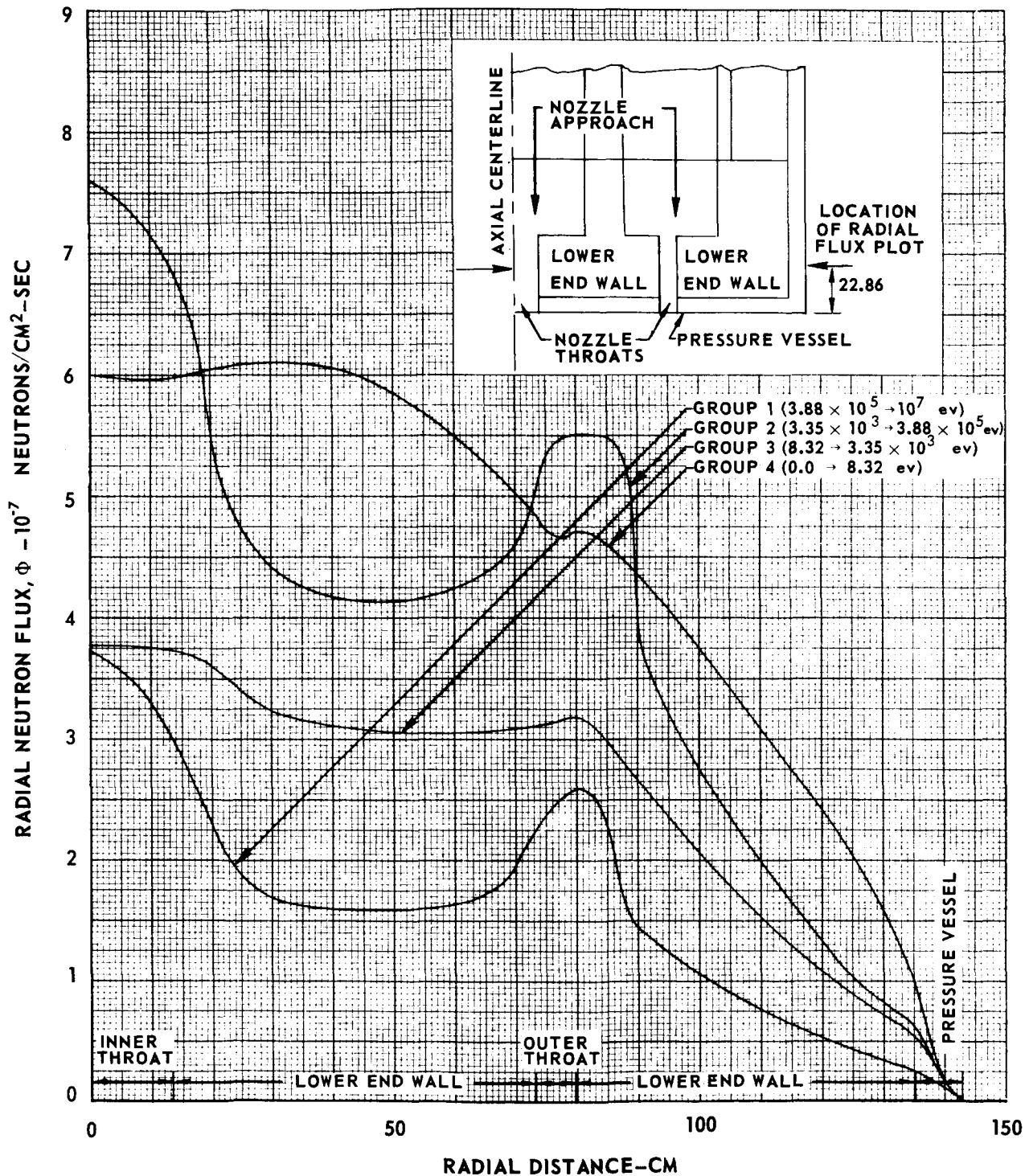
BASIC SPHERICAL GEOMETRY USED IN ONE-DIMENSIONAL, 24-GROUP, S4 CALCULATIONS FOR OPEN-CYCLE ENGINE

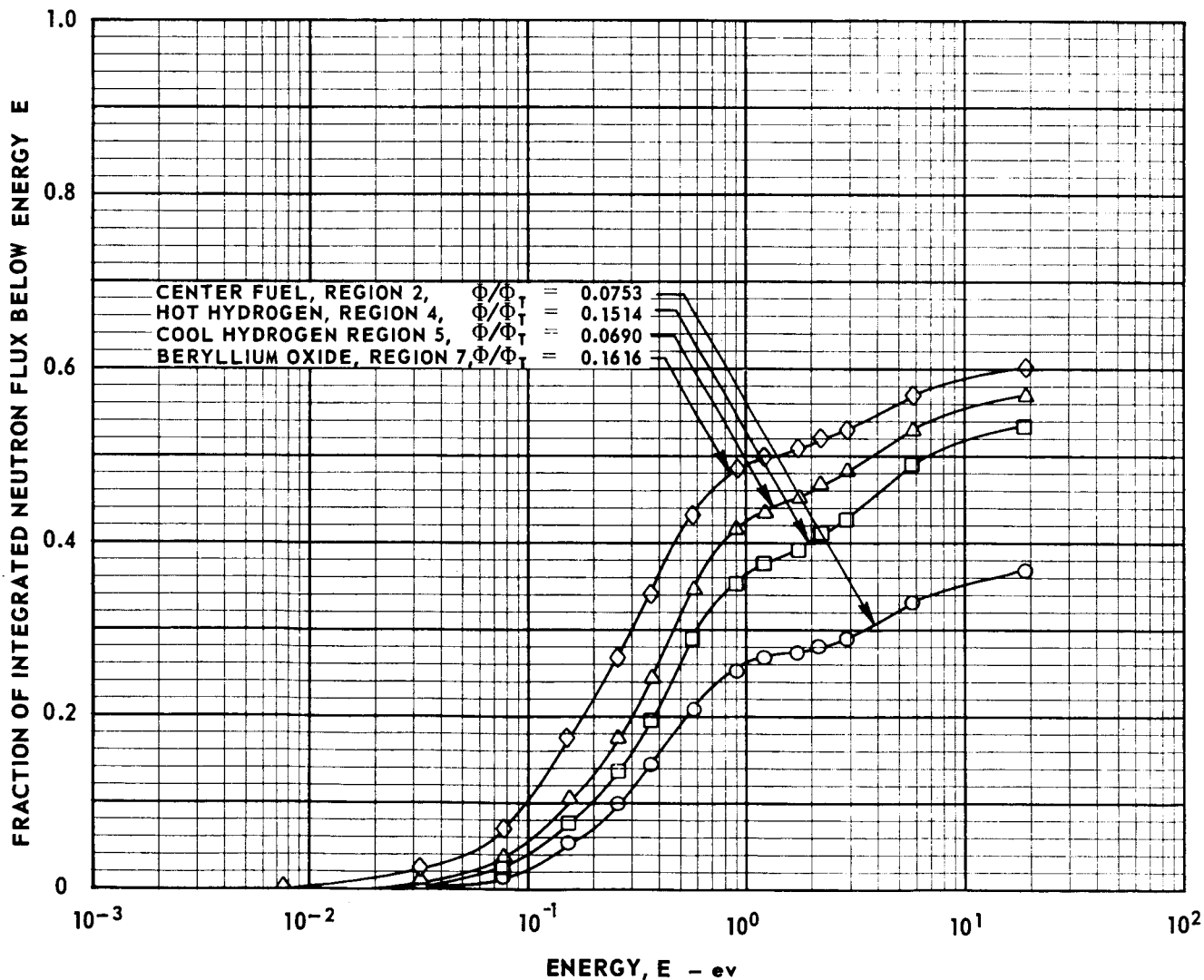CIRCLED NUMBERS INDICATE REGIONS DESCRIBED IN TABLES XIV AND XV

ALL DIMENSIONS IN CM

INTEGRATED FLUXES FROM ONE-DIMENSIONAL, 24-GROUP
S4 CALCULATIONS FOR OPEN-CYCLE ENGINE

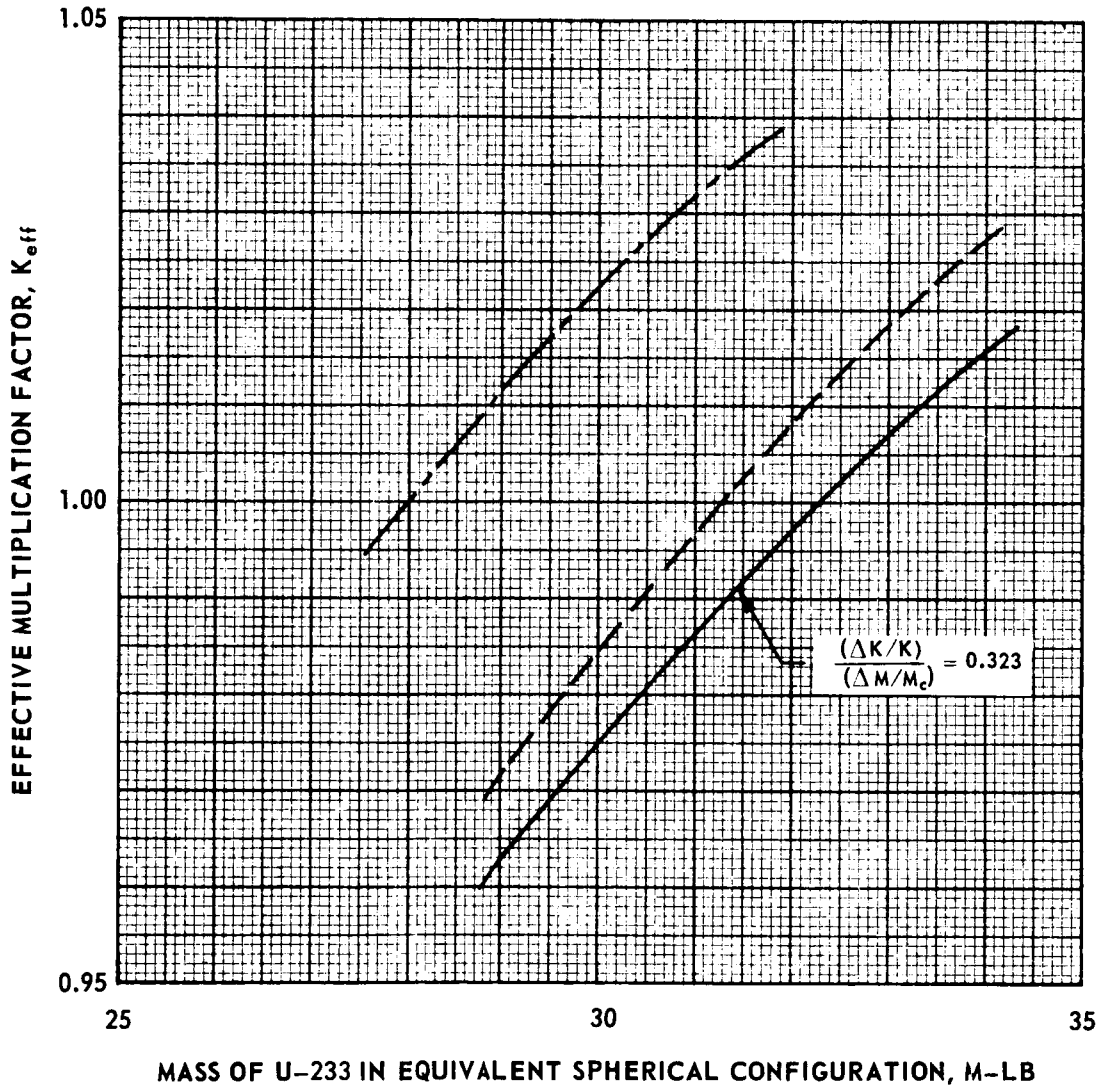DESCRIPTION OF CONFIGURATION GIVEN IN TABLES XIV AND XV AND FIG. 13

STEPPED FUEL DENSITY PROFILE USED AS DESCRIBED IN FIG. 6 OF REF. 1

U-233 CRITICAL MASS DETERMINATION FROM ONE-DIMENSIONAL 24-GROUP CALCULATIONS FOR EQUIVALENT SPHERICAL CONFIGURATION FOR OPEN-CYCLE ENGINE

DESCRIPTION OF CONFIGURATION GIVEN IN TABLES XIV AND XV AND FIG. 13

STEPPED FUEL DENSITY PROFILE USED AS DESCRIBED IN FIG. 6 OF REF. 1

LINE	CASE	1-D, M_c -LB	EQUIVALENT 2-D, M_c -LB
— · —	DIFFUSION THEORY	28.01	32.50
— — —	DIFFUSION THEORY CORRECTED FOR H_2 COOLANT IN REFLECTOR-MODERATOR	31.30	36.30
———	S_4 TRANSPORT THEORY	32.30	37.50

$$\frac{(\Delta K/K)}{(\Delta M/M_c)} = 0.323$$

EFFECTIVE MULTIPLICATION FACTOR, K_{eff}

MASS OF U-233 IN EQUIVALENT SPHERICAL CONFIGURATION, M-LB

COMPARISON OF INTEGRATED U—233 FISSION NEUTRON SOURCES
FROM ONE-DIMENSIONAL, 24—GROUP, S4 CALCULATIONS
FOR NUCLEAR LIGHT BULB AND OPEN-CYCLE ENGINE

FISSION NEUTRON SOURCES NORMALIZED SUCH THAT PRODUCTION IN FUEL REGIONS = 1 NEUTRON/SEC

DESCRIPTION OF NUCLEAR LIGHT BULB CONFIGURATION   GIVEN IN TABLES I TO V AND FIG. 3

DESCRIPTION OF OPEN-CYCLE CONFIGURATION GIVEN IN TABLES XIV AND XV AND FIG. 13